Millennial-scale deglaciation across the European Alps at the transition between the Younger Dryas and the Early Holocene - evidence from a new cosmogenic nuclide chronology

Marie Protin, Irene Schimmelpfennig, Jean-louis Mugnier, Jean-françois Buoncristiani, Melaine Le Roy, Benjamin Pohl, Luc Moreau

Millennial-scale deglaciation across the European Alps at the transition between the Younger Dryas and the Early Holocene – evidence from a new cosmogenic nuclide chronology

Marie Protin, Irene Schimmelpfennig, Jean-Louis Mugnier, Jean-François Buoncristiani, Melaine Le Roy, Benjamin Pohl, Luc Moreau and ASTER Team

The reconstruction of mountain glacier response to rapid climate change in the past allows accessing the effects of current climate change. Yet, the spatial and temporal variability of past glacier fluctuations is not fully understood. In this study, we address the timing of glacier fluctuations in the European Alps during the Younger Dryas/Early Holocene (YD/EH) transition. In an effort to elucidate whether glacier fluctuations were synchronous during this period, we present a new chronology of the Alpine Talèfre glacier, based on 14 new *in situ*-produced cosmogenic ^{10}Be ages of moraines and roches moutonnées. The retreat of Talèfre glacier was initiated during the mid-YD (~12.4 ka), then it experienced a gradual retreat punctuated by at least 3 oscillations until ~11 ka before shrinking substantially within its Little Ice Age limits (13th-19th century). Comparison of our findings with published glacier chronologies in the Alpine region highlights broadly synchronous behavior of glaciers across the Alps between 12 and 10 ka. The coeval glacier fluctuations at a regional scale suggest that common regional climate conditions had a major impact on Alpine glacier variations during the YD/EH transition. The similarity of glacier behavior and independent temperature records in both the Alpine region and the Northern high latitudes suggests a teleconnection between these regions, but differences in the amplitude of the mean annual versus summer temperature signals point to pronounced changes in seasonality between the YD and the EH.

Keywords

Younger Dryas/Early Holocene transition; European Alps; Cosmogenic nuclide dating; Glacier fluctuations.

Marie Protin [marie.protin@univ-lorraine.fr], Aix-Marseille Univ, CNRS, IRD, INRA, Coll France, CEREGE, Aix en Provence, France and Université de Lorraine, CNRS, CRPG, F-54000 Nancy, France ; Irene Schimmelpfennig [schimmelpfennig@cerege.fr] and ASTER Team (Georges Aumaître [aumaitre@cerege.fr], Didier Bourlès, [bourles@cerege.fr], Karim Keddadouche [keddadouche@cerege.fr]), Aix-Marseille Univ, CNRS, IRD, INRA, Coll France, CEREGE, Aix en Provence, France; Jean-Louis Mugnier [jean-louis.mugnier@univ-smb.fr], Université Grenoble Alpes, Université Savoie Mont Blanc, CNRS, ISTerre, 73000 Chambéry, France ; Jean-François Buoncristiani [jfbuon@u-bourgogne.fr] and Benjamin Pohl [benjamin.pohl@u-bourgogne.fr], Biogéosciences, UMR 6282 CNRS, Université Bourgogne Franche-Comté, 6 Boulevard Gabriel, 21000 Dijon, France ; Melaine Le Roy [melaine.leroy@unige.ch], University of Geneva, Institute for Environmental Sciences, Climate Change Impacts and Risks in the Anthropocene (C-CIA), CH-1205 Geneva, Switzerland and Université Grenoble Alpes, Université Savoie Mont Blanc, CNRS, EDYTEM, 73000 Chambéry, France ; Luc Moreau [moreauluc@chx.fr], Université Grenoble Alpes, Université Savoie Mont Blanc, CNRS, EDYTEM, 73000 Chambéry, France.

Mountain glaciers are recognized as sensitive recorders of climate variability, and their fluctuations mainly depend on variations of both temperature during the melt season and snowy precipitation (Oerlemans, 2005; Roe et al., 2017). In t~~T~~he case of~~ the~~ alpine glaciers, their recent evolution shows that it ~~their recent evolution ~~is controlled by large scale climate variations moderated by local specific factors (Rabatel et al., 2013; Vincent et al., 2017). In the light of current climate evolution and rapid retreat of glaciers worldwide, it is important to improve our understanding of the sensitivity of glaciers to rapid climate changes in the past, such as those during the Younger Dryas/Early Holocene (YD/EH) transition (between ~12 to 10 ka). Therefore, the impact of large-scale climate variations versus local climate and site-specific factors has to be better assessed by constraining past glacial chronologies.

Commenté [MLR1]: Si tu parles des Alpes il faut mettre une majuscule à Alpine ici … sinon ça désigne les glaciers de montagne en général

Moraines and roches moutonnées represent clear geomorphic markers of past glacier extents. Studying and dating them is a valuable approach for constraining former glacier behavior, establishing glacier chronologies and investigating the related climate changes. Due to the lack of direct dating methods, the traditional chronology of glacier advances ("stadials") in the Alps during the period of Late-Glacial and Early Holocene (EH) deglaciation is mainly based on comparative studies of moraine stratigraphies and morphologies and equilibrium line altitude (ELA) determinations (e.g. Maisch, 1981). The temporal correlations of these stadials with paleoclimatic periods were broadly confirmed by the pioneering cosmogenic nuclide studies at a few Alpine sites (see reviews in Ivy-Ochs, 2015; Ivy-Ochs et al., 2006). For instance, the Egesen stadial moraines are assigned to the Younger Dryas (YD) (from 12.9 to 11.7 ka; Rasmussen et al., 2006), and are associated with an ELA depression of 250-350m relative to the Little Ice Age (LIA) (Ivy-Ochs, 2015). The Kartell stadial moraines are assigned to the Preboreal cold oscillation (11.4 – 11.3 ka; Kobashi et al., 2008) with an ELA depression of 120m (Ivy-Ochs, 2015). However, recent studies showed that correlating moraines from different Alpine valleys solely based on the above-mentioned comparative criteria only is not

Commenté [MOU2]: Non, il faut pas rajouter ça, on a déjà « solely » dans la phrase reliable, highlighting the need for direct moraine dating with cosmogenic nuclides when comparing moraines from various sites (e.g. Boxleitner et al., 2019; Reitner et al., 2016). Over the past few years, parameters for the calculations of cosmic ray exposure ages were refined (e.g. Balco, 2017; Balco et al., 2009, 2008; Borchers et al., 2016; Martin et al., 2017; Young et al., 2013) and an increasing number of cosmogenic nuclide dating studies from the Alps have been published, providing evidence of multiple glacier fluctuations during the Late-Glacial and the EH (e.g. Baroni et al., 2017; Moran et al., 2016b, 2016a; Schindelwig et al., 2012). Attempts of identifying temporal or spatial trends in Alpine glacier behavior during the Late-Glacial and EH have been made in earlier studies (Braumann et al., 2020; Chenet et al., 2016; Schimmelpfennig et al., 2014). Although age uncertainties are generally too large to infer clear trends, an abrupt glacier recession is not documented in the Alps at the very sharp transition between YD and Holocene that is observed in Greenland ice cores with a ~10°C warming in less than one hundred years~~-~~.

Rather, previous studies suggested that EH glacier stillstands or advances in the Alps could be a response to abrupt cold spells observed in Greenland ice cores (e.g. Ivy-Ochs et al., 2009; Schimmelpfennig et al., 2014, 2012; Schindelwig et al., 2012), such as the Preboreal Oscillation or a cold event notable at ~10.9 ka (Rasmussen et al., 2006; Vinther et al., 2006).

In the Western ~~part of the mountain range~~Alps, ~~Alpine~~ glacier chronologies from this period have for a long time been very scarce, but recent robust records and additional data from the French Alps will now provide the opportunity to use the Alpine data set as a whole for a regional analysis (Chenet et al., 2016; Cossart et al., 2012; Hofmann, 2018; Protin et al., 2019; Schimmelpfennig et al., 2019; Le Roy et al., in prep). The chronological investigation of these moraine chronologies might indeed allow for a better understanding of the large-scale paleoclimatic conditions during a period for which proxy and model data still show diverging temperature trends in both mid- and high latitudes: coupled ocean-atmosphere climate models

Commenté [MOU3]: Marie, l'ordre des citations suit normalement des règles strictes, à voir en fonction du journal – à vérifier de partout dans le texte (tu les as mis toujours dans l'ordre alphabétqiue, c'est sûr que c'est bon ?)

Commenté [MOU4]: C'est pas d'abord 2012,

Commenté [MLR5]: Je ne sais pas si tu peux citer ça ;;;

Commenté [MOU6R5]: Sinon, il faut citer notre poster Schimmelpfennig et al., 2019 (e.g. Buizert et al., 2014) failed to reproduce the abrupt warming at the end of the YD found in North Atlantic and Greenland ice cores (e.g. Rasmussen et al., 2006; Shakun et al., 2015), whereas continental temperature reconstructions based on biological proxies either fit with this drastic warming (chironomid records in Heiri et al., 2015) or indicate a much more gradual warming (e.g. pollen records in Marsicek et al., 2018; glacier chronologies in Rainsley et al. 2018, Young et al., 2020).

In this study, we provide a new glacier chronology in the French Alps by analyzing the Talèfre glacier patterns during the deglaciation of the "Jardin de Talèfre", one of the highest moraine sites in the Alps (close to 3000 m) where a set of moraines is deposited above roches moutonées. We present new *in-situ* cosmogenic beryllium-10 (^{10}Be) ages of moraines and roches moutonnées for this zone (Fig. 1Fig. 1) and compare these new data with published ^{10}Be glacial chronologies from elsewhere in the European Alps, selected for their quality (e.g. number of samples, dispersion of the ages) and re-calculated using uniform methods. Building on this regional compilation, we evaluate (i) the possibility of a regional synchroneity of glacier fluctuations during the multi-millennia period of the end of the YD and the beginning of the Holocene (hereafter YD/EH transition), (ii) the impact of large-scale climate variations on glacier patterns versus site-specific factors, (iii) the underlying climatic drivers in a regional scale and their potential link with the high-latitudes, and (iv) the climatic significance of the small fluctuation range of glacier extent between the YD and EH in the light of the significant and abrupt climate change recorded in independent proxy records.

Study site

Talèfre glacier (45°54'N, 6°59'E) is a cirque glacier located in the French part of the Mont-Blanc massif and wasis a major tributary of Mer de Glace glacier, the largest glacier in the Mont-Blanc massif (Fig. 1Fig. 1). To the north is located the Argentière glacier, the second largest glacier in the Mont-Blanc massif (Fig. 1~~Fig. 1~~). In 2008, Talèfre glacier covered an area of ~8 km^2 with a maximum length of 4.5 km and altitude spanning 2473 m to 3743 m a.s.l. (Gardent, 2014). The ELA of Talèfre glacier for the period 1984-2010 was estimated to ~3000 m (Rabatel et al., 2013). Next to Argentière glacier, the mean annual temperature and precipitation for the time period 1979-2002 are estimated at 1.8°C and 1783 mm at ~2000 m a.s.l. (Joly et al., 2018 and personal communication of D. Joly). The catchment of Talèfre glacier is ~~constrained~~ bordered by ~~hillsides~~ rock faces composed of granite rocks of late Hercynian age (~300 Ma; Bussy et al., 2000).

During the YD, Talefre glacier was connected to Mer de glace, which at that time occupied the Arve Valley with a front located westward of the left boundary of Fig. 1~~Fig. 1~~ (Prud'homme et al., 2020). During the last LIA advance in the 19th century, Talèfre glacier was confluent with Leschaux glacier, which then joins Tacul glacier to form Mer de Glace (Fig. 1~~Fig. 1~~). Since ~1950 the Talèfre and Leschaux glaciers have not been coalescing (Gardent, 2014).

A notable feature of Talèfre glacier is the presence of a triangle-shaped rock islet at its center, named "Jardin de Talèfre" (i.e. Talèfre garden). This islet is bounded by moraines (

Commenté [MLR7]: La référence à citer pour le front de la MdG pendant le PAG est plutôt Nussbaumer et al 2007

Commenté [MOU8R7]: ? Mais ici on parle du YD… donc je pense que tu peux laiisser comme ça

Commenté [MOU9]: Better « further downvalley »?

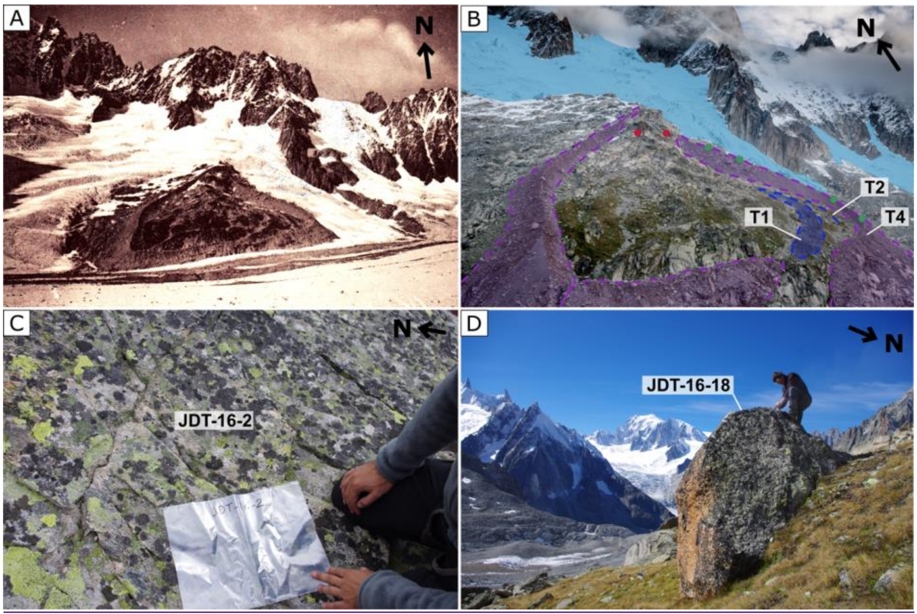

Fig. 2~~Fig. 2~~), that span 2640 m to 3040 m a.s.l. (Jordan, 2010). Because of its remoteness, this area has not been disturbed by human activity. According to the French État-Major maps (surveyed in 1820-1866) and first available photographs made by August-Rosalie Bisson in 1862 the “Jardin de Talèfre” was not ice-covered during the last LIA maximum (de Decker Heftler, 2002).

Methodology

Moraine mapping

Several so-far undated moraine ridges preserved on the islet were studied and represented in the geomorphologic map of

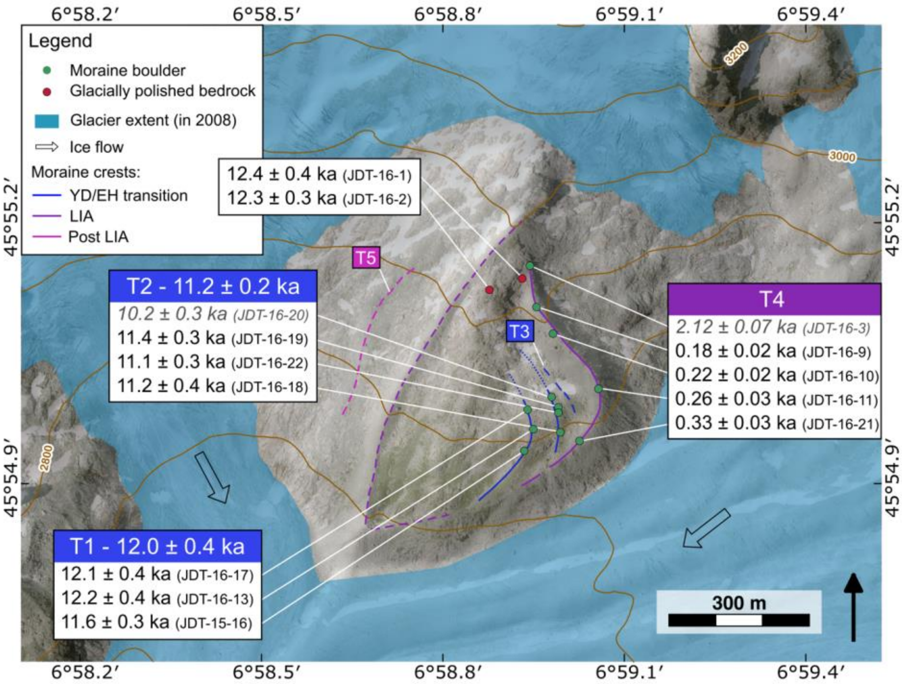

Fig. 3~~Fig. 3~~. The mapping was realized through field work and interpretation of aerial images from the year 2015 (French national institute of geographic and forest information - IGN, 50 cm resolution).

Sample collection

Fourteen samples were collected in the "Jardin de Talèfre", two from smoothed bedrock surfaces resulting from glacial erosion and 12 from moraine boulders (

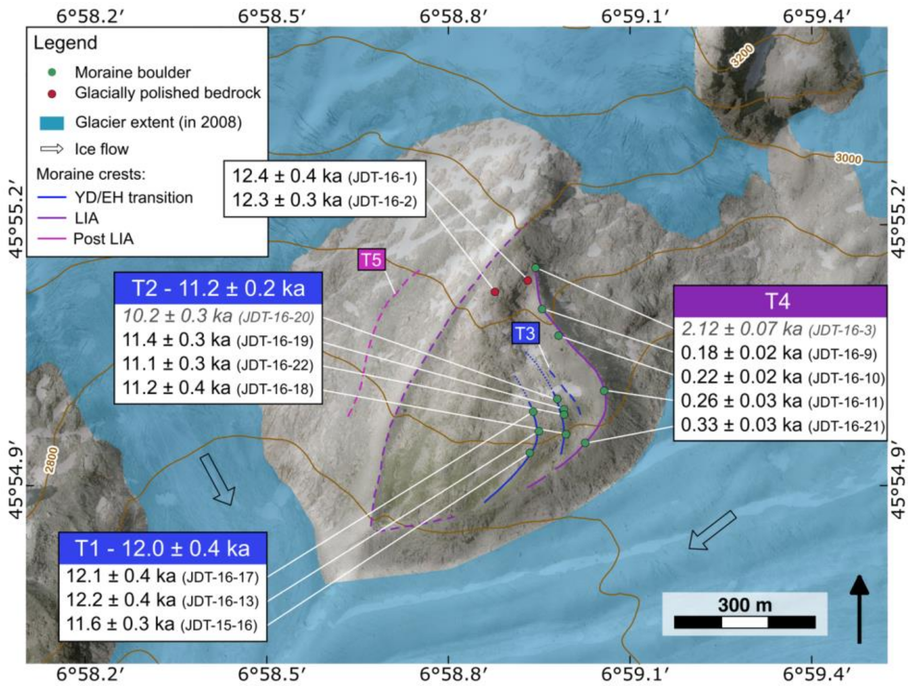

Fig. 3Fig. 3). Bedrock samples were taken from the surface of the rocky islet, and attention was paid to avoid the possibility of cover by snow or vegetation and significant erosion by choosing sloping spots with glacial morphologies (

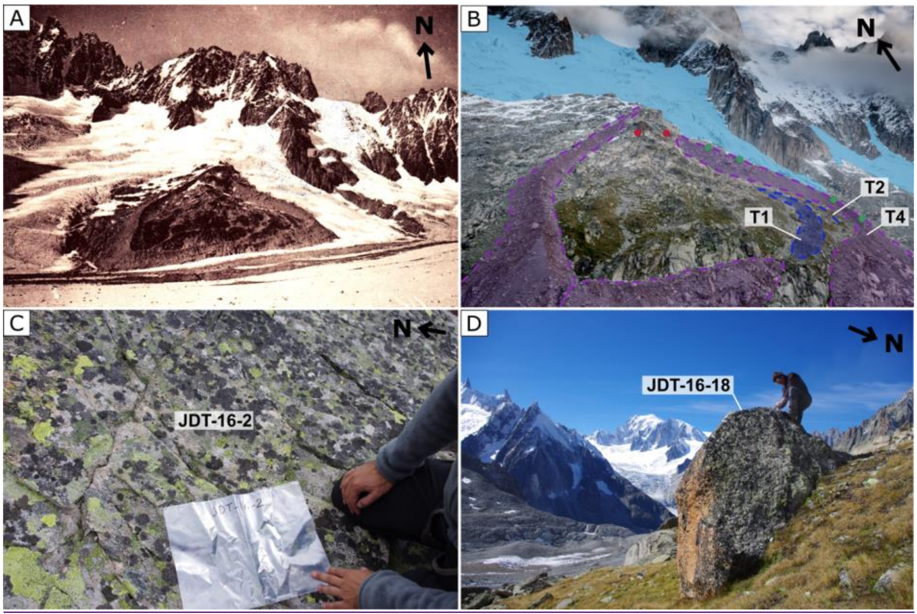

Fig. 2~~Fig. 2~~c). Both surfaces were covered by lichen. Moraine boulder samples were taken from the top of the boulders, which were embedded in the crest or slope of the targeted moraines (

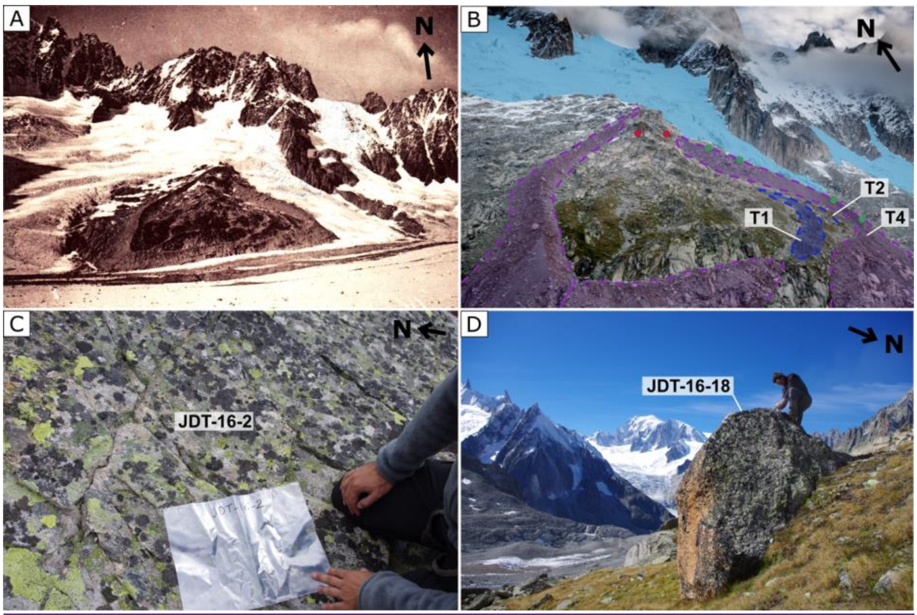

Fig. 2Fig. 2d). If we assume uninterrupted surface exposure, the bedrock exposure ages indicate when the “Jardin de Talèfre” became ice-free for the last time, while the boulder exposure ages represent the timing of the glacier culmination and moraine stabilization (for detailed discussion see section “Oscillation of Talèfre glacier since the Younger Dryas”). Samples were collected using a chisel, a hammer and a cordless angle grinder, and topographic shielding was evaluated in the field using a clinometer.

Laboratory procedures

All samples were processed at CEREGE (Aix-en-Provence, France). Samples were crushed and sieved to collect the 250-500 µm fraction. Quartz was first concentrated by magnetic separation and then isolated by successive leaching in a H_2SiF_6/HCl mixture or by froth flotation when the mineralogy allowed it. The obtained quartz fraction was leached at least two times in a 5% HF - 5% HNO_3 solution, followed by 24h in ultra-sonic baths in a 1% HF - 1% HNO_3 solution in order to remove any remaining feldspars and to clean the grains from atmospheric ^{10}Be. Purified quartz was completely dissolved in concentrated HF after addition of ~0.1 g of an in-house ^{9}Be carrier solution (3025 ± 9 ppm; Merchel et al., 2008). Beryllium was extracted by successive alkaline precipitations of $Be(OH)_2$ alternated with separation on anion and cation columns. Samples were then oxidized at 700°C for one hour and the final BeO mixed with Nb powder and loaded into nickel cathodes. Measurements of the $^{10}Be/^{9}Be$ ratios by accelerator mass spectrometry (AMS) were conducted at the French national AMS facility ASTER (Arnold et al., 2010). Samples were calibrated against in-house standard STD-11 with a ($^{10}Be/^{9}Be$ ratio of= (1.191 ± 0.013) $\times 10^{-11}$; (Braucher et al., 2015)) and a ^{10}Be half-life of (1.387 ± 0.0012) $\times 10^{6}$ years (Chmeleff et al., 2010; Korschinek et al., 2010). Analytical uncertainties combine ASTER counting statistics and stability (~5%; Arnold et al., 2010) and machine blank correction. The number of atoms ^{10}Be in the samples calculated from the corresponding ^{10}Be/^{9}Be ratios was then corrected from that of the chemical blanks, which had ^{10}Be/^{9}Be ratios of 3.38 ± 0.49 x10^{-15} and 3.48 ± 0.50 x10^{-15} (Table 1~~Table 1~~).

Age calculations

Surface exposure ages of the here presented new data were computed with the CREp online calculator (Martin et al., 2017) using the Lal-Stone time corrected scaling scheme Lm, the ERA40 atmospheric reanalyses and the Atmospheric ^{10}Be-based VDM for geomagnetic database (see Martin et al., 2017 and references therein). We applied the production rate of 4.10 ± 0.10 atoms ^{10}Be.g^{-1}.a^{-1} established by Claude et al. (2014) as it is the only regional ^{10}Be production rate available for Alpine sites and it is identical to the global ^{10}Be production rate resulting from the ICE-D database linked to CREp (4.11 ± 0.19 atoms ^{10}Be.g^{-1}.a^{-1}). The two other production rates often used for studies in the Alps, i.e. the northeast North America "NENA" production rate (Balco et al., 2009) and the "Arctic" production rate (Young et al., 2013), which is almost identical with the recent Scotland production rate (Putnam et al., 2019), would lead to ages older by less than 2% and 1%, respectively. For easy comparison, we present in Table 1 the ages calculated with both the regional regional production rate and the "Arctic" production rate. We did not apply a correction for snow shielding, as we do not have sufficient quantitative data on snowfall during the Holocene, and all sampled surfaces are in wind-exposed locations. We did not correct for potential erosion, as we were careful to sample surfaces with least possible erosion. Applying a correction for considerable snow cover assuming 50 cm of snow for six months (Chenet et al., 2016) would lead to ages older by 6% to 8%. Applying a correction for erosion corresponding to an erosion rate of 1 mm.kr^{-1} (André, 2002) would result in ages older by less than 1%.

Commenté [MOU10]: Needs to be added in the table

For the regional comparison of glacier records, previously published data from 18 study sites (see references in Fig. 6) were homogenized by re-calculating the individual and mean ages using the same procedures as above (Table S1). Boulders identified as outliers in the original studies were kept as outliers. Applying the χ^2 test (2σ) by Ward and Wilson (1978)~~above-mentioned χ^2 test~~, moraine age populations were tested for outliers, which were also discarded as indicated in Table S1. Exceptions were made for the moraine M7a from the Rougnoux valley, M2 from Falgin cirque and the lower moraine from Steingletscher, where all boulders (not identified as outliers by authors) were kept for the mean age calculation even if they statistically mismatch, as we do not have any argument for discarding a specific sample from the age population. At the Rougnoux valley site, several moraine mean ages do not agree with the stratigraphic order (M8-9, M7b, M4-5 and M6b) but these ages do not statistically differ; therefore, we choose to include them all in the comparison. We eliminated from the comparison the moraine ages that are based on only one sample and that have standard deviations >10% to make the comparison as accurate as possible. Once this selection made, only the sites with at least one moraine of Holocene age (< 11.7 ka) were kept for the comparison in order to exclude sites with moraines that exclusively correspond to earlier Late-Glacial advances. Boxleitner et al. (2019) dated 34 moraine boulders of several glacier systems in Meiental (central Alps), but we deliberately did not consider the study in our test, because each moraine was dated with only one boulder. Applying a realistic snow cover correction to all sites would equally shift all moraine ages to slightly older dates and would not change the discussion.

Results

Geomorphologic description of the Talèfre site

Two massive lateral moraines, up to 50m high and 1km long, frame the islet of the “Jardin de Talèfre” (purple moraines, including T4, in

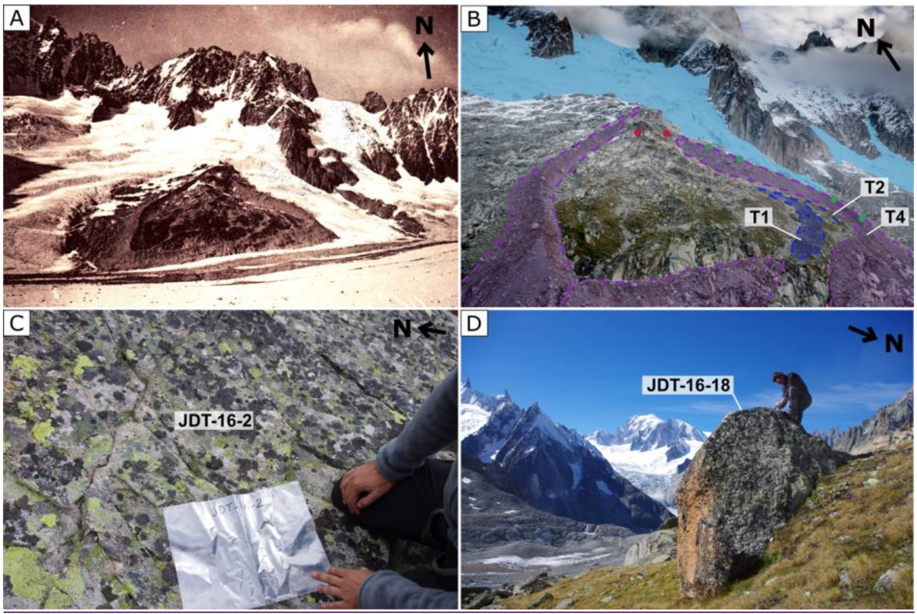

Fig. 2~~Fig. 2~~b and

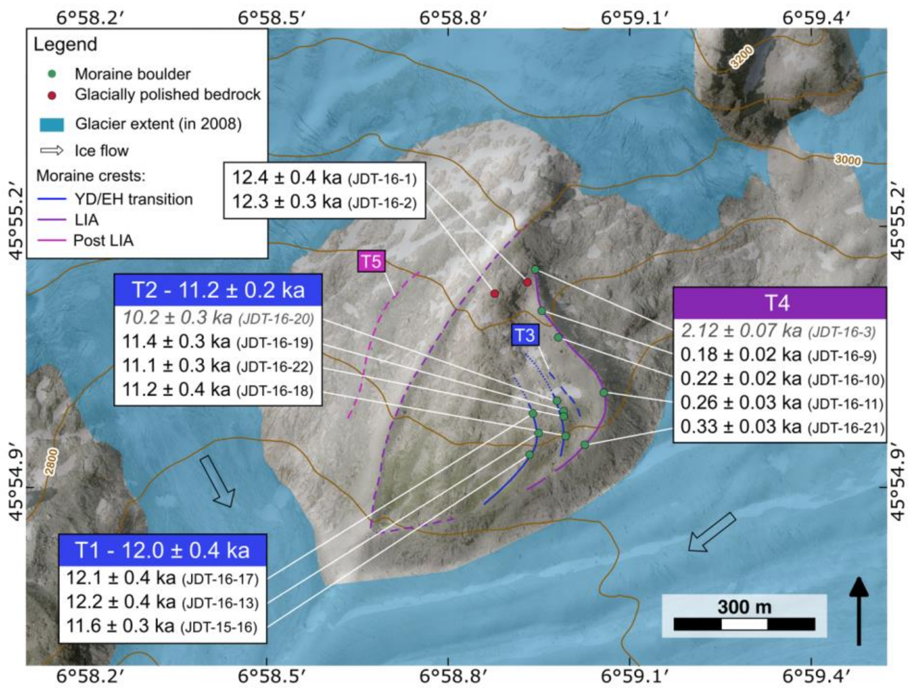

Fig. 3Fig. 3). In the eastern part of the islet, three very smooth lateral moraine ridges (T1, T2 and T3) are visible in stratigraphically older location relative to the massive moraine T4 on the eastern margin. They are less than 2m high and between 100 and 200m long. The two outermost of these three moraine ridges (T1 and T2) bear several large boulders suitable for ^{10}Be dating, while the ridge T3 does not. These three ridges (T1 to T3) are represented in dark blue in

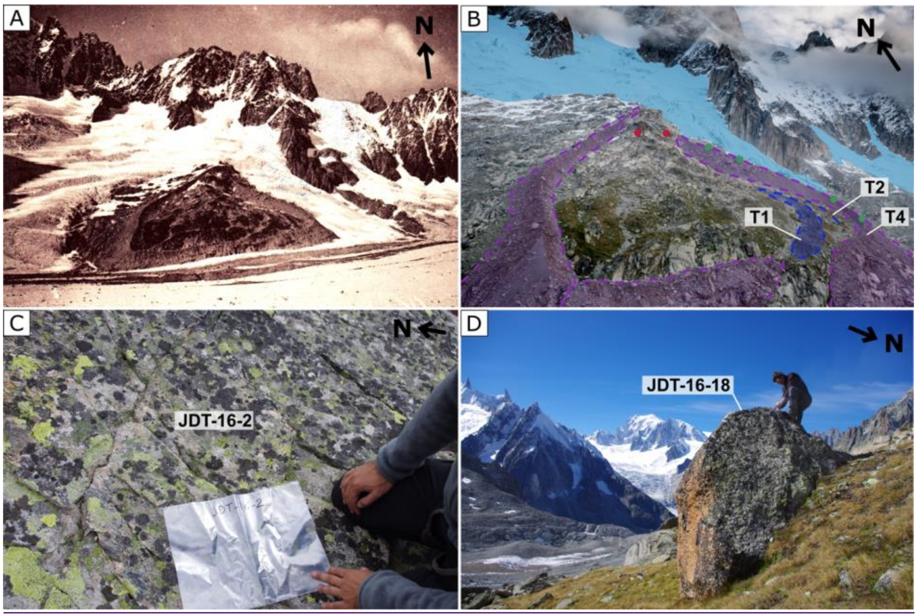

Fig. 2Fig. 2b and

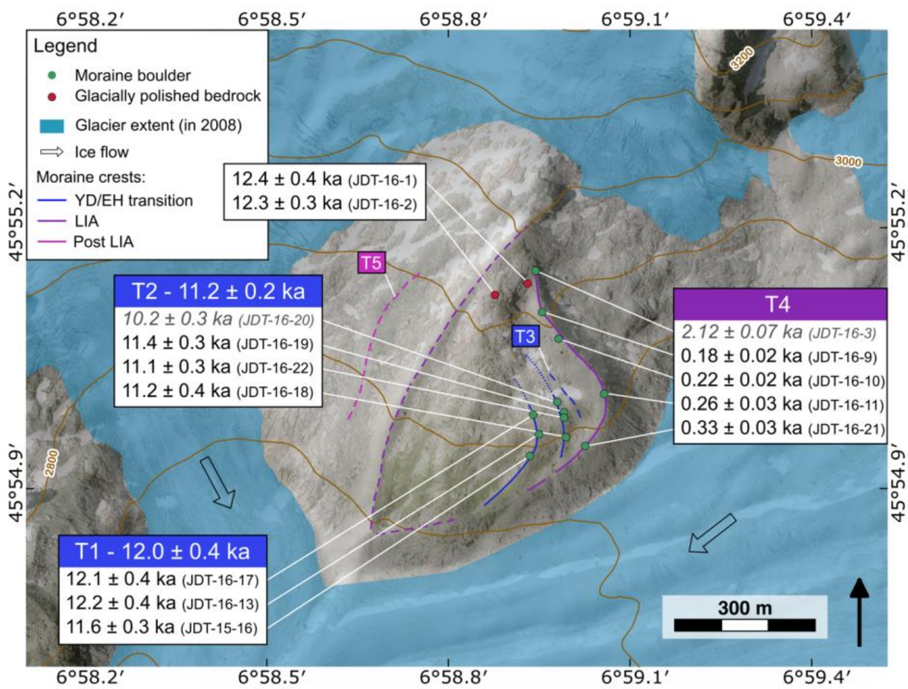

Fig. 3Fig. 3. Moraine mapping shows that they are leaning northward against a 20 m high rock slope at an altitude of ~2850m a.s.l.; to the south, they are crosscutted by the T4 moraine. Between the western massive ridge and the present glacier margin, a small ridge (T5) is visible (pink moraine in

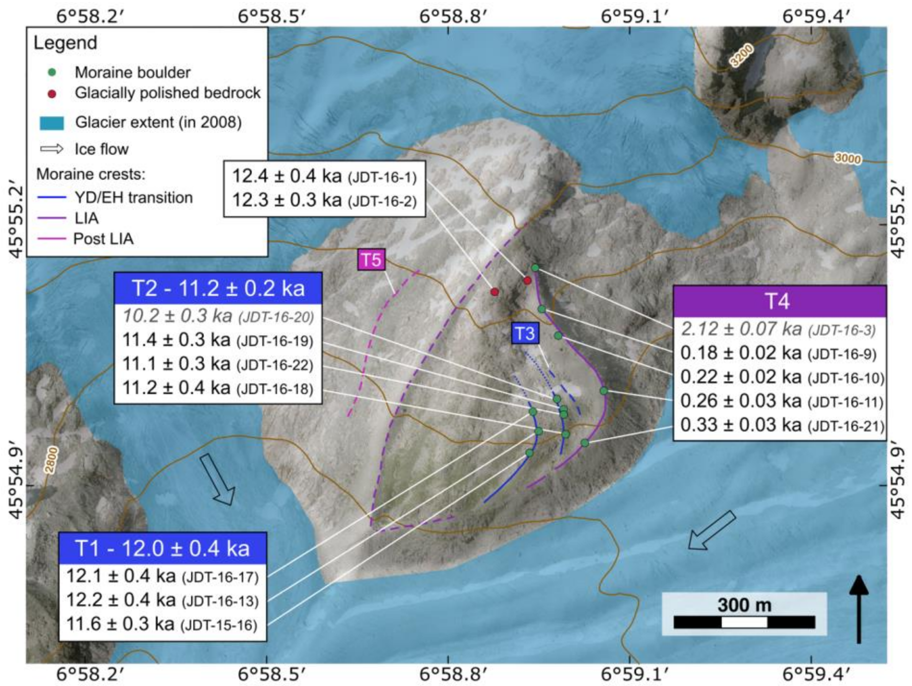

Fig. 3~~Fig. 3~~). It has no equivalent on the eastern side and has been probably deposited during one of the short advances/stillstands that occurred at Alpine sites during the general glacier retreat of the 20th century (Braumann et al., 2020; Schimmelpfennig et al., 2014).

Moraine and bedrock exposure ages of Talèfre glacier

The two bedrock surfaces were sampled at the center of the northern part of “Jardin de Talèfre”. Moraine boulder samples were taken from three ridges in the eastern part of the islet, i.e. from the two stratigraphically outermost (oldest), smooth moraines T1 and T2, and from the innermost (youngest), massive moraine T4. Surface exposure ages are shown in

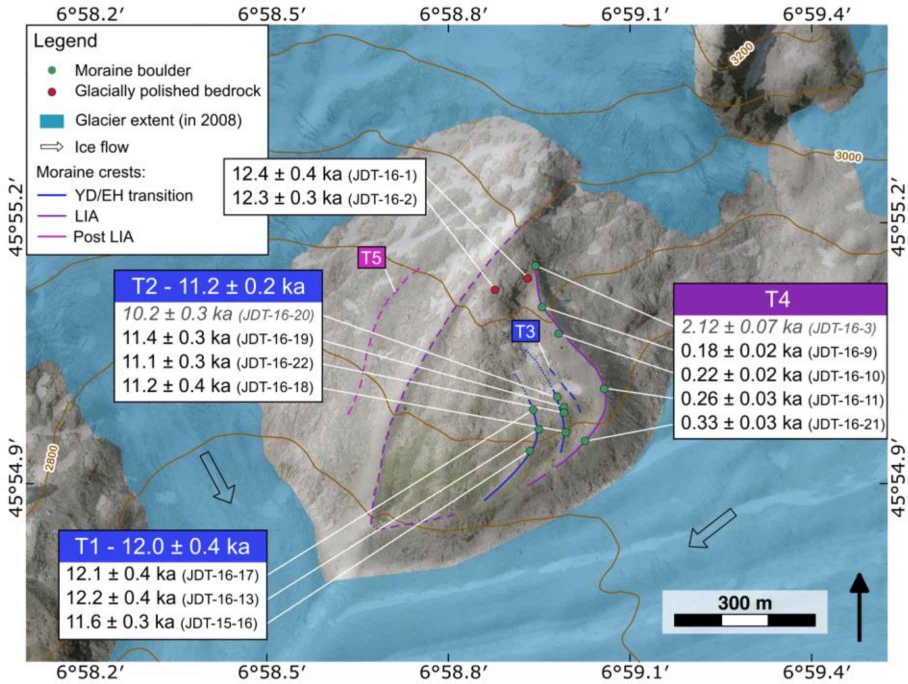

Fig. 3~~Fig. 3~~ and detailed in Table 1~~Table 1~~. Probability plots of moraine boulder ages and arithmetic mean ages are shown in

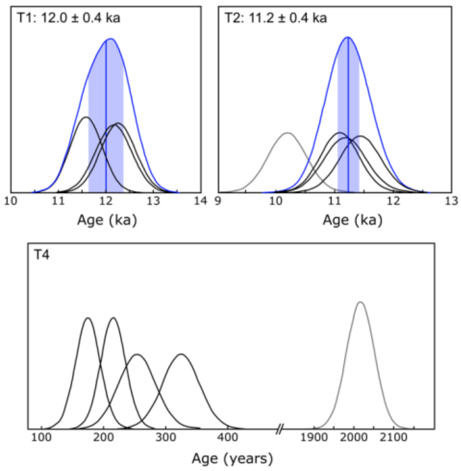

Fig. 4~~Fig. 4~~. The consistency of individual ages within one moraine age populations were tested for outliers with the χ^2 test (2σ) by Ward and Wilson (1978), using the analytical uncertainties of the ages. In the text and in figures, individual ages are given with the analytical uncertainties, to allow for internal comparison, and arithmetic mean ages are given with their standard deviations, while Table 1 shows both analytical uncertainties and total uncertainties (including the ^{10}Be rate uncertainty). See figure and table captions for details.

All ages are in agreement with their stratigraphic order. The two bedrock samples, JDT-16-1 and JDT-16-2, give indistinguishable exposure ages of 12.4 ± 0.4 ka and 12.3 ± 0.3 ka, respectively. The three boulder ages from the outermost moraine T1 range between 12.2 ± 0.4 ka and 11.6 ± 0.3 ka, with a mean age of 12.0 ± 0.4 ka. Three boulder ages from moraine T2 are very well clustered between 11.4 ± 0.3 ka and 11.1 ± 0.3 ka and give a mean age of 11.2 ± 0.2 ka after discarding JDT-16-20 as an outlier (10.2 ± 0.3 ka). This boulder is less than 1m high. It might thus have been exhumed or covered for a while by a layer of sediment, leading to an underestimation of its exposure age. On the innermost moraine, four boulders yield ages of 0.18 ± 0.02 ka, 0.22 ± 0.03 ka, 0.26 ± 0.02 ka and 0.33 ± 0.03 ka and one boulder is dated at 2.12 ± 0.07 ka.

According to this new set of exposure ages we propose a reconstruction of the past extents of Talèfre glacier, corresponding to moraines T1 and T4 (

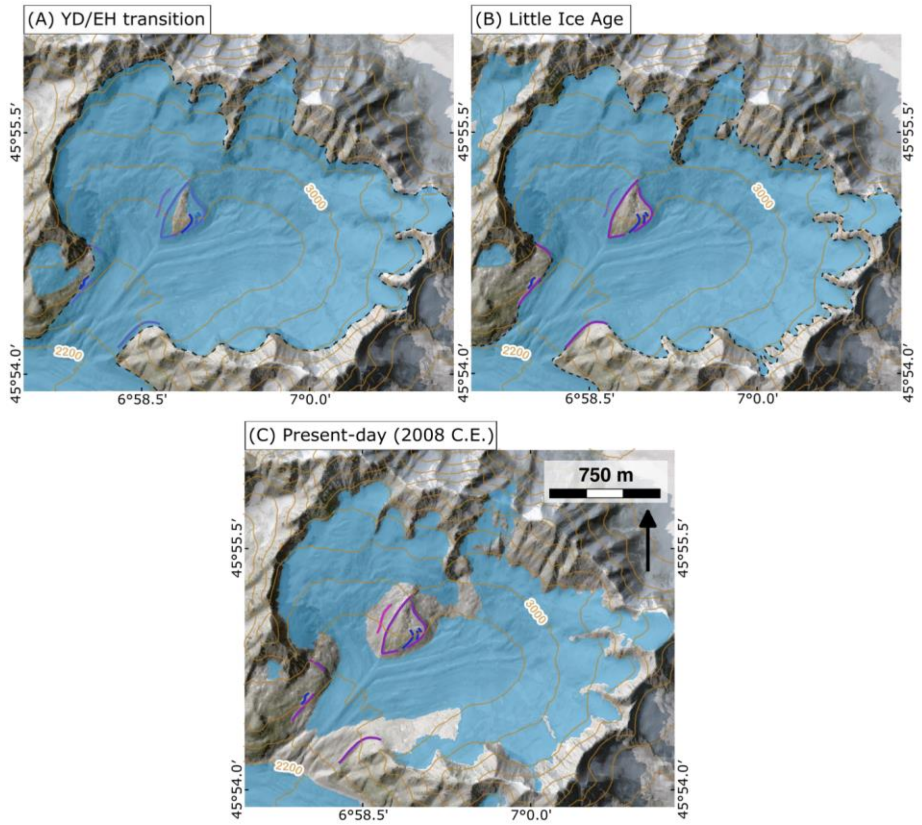

Fig. 5Fig. 5). The mapping of the exterior glacier margins relies solely on remnants of undated moraines, assumed variations in relation to catchment slopes and 19th century maps from French État-Major.

Exposure ages of the other Alpine chronologies

The previously published 18 Alpine glacier chronologies that are considered here, are characterized by sets of lateral and/or latero-frontal moraines originally dated between ~13.5 ka and ~9.5 ka. Of these 18 sites, eleven meet the quality criteria presented in the Methodology (see section "Age calculations") and yield recalculated ^{10}Be exposure ages between 14.5 ka and 9.8 ka ka. The moraine ages of the other sites are either older (Val Viola, Gesso della Barra valley, Romanche valley, Great Aletsch glacier, Ferwall site) or show large standard deviations (Clarée valley). Probability curves for all retained moraine mean ages in each site are plotted in

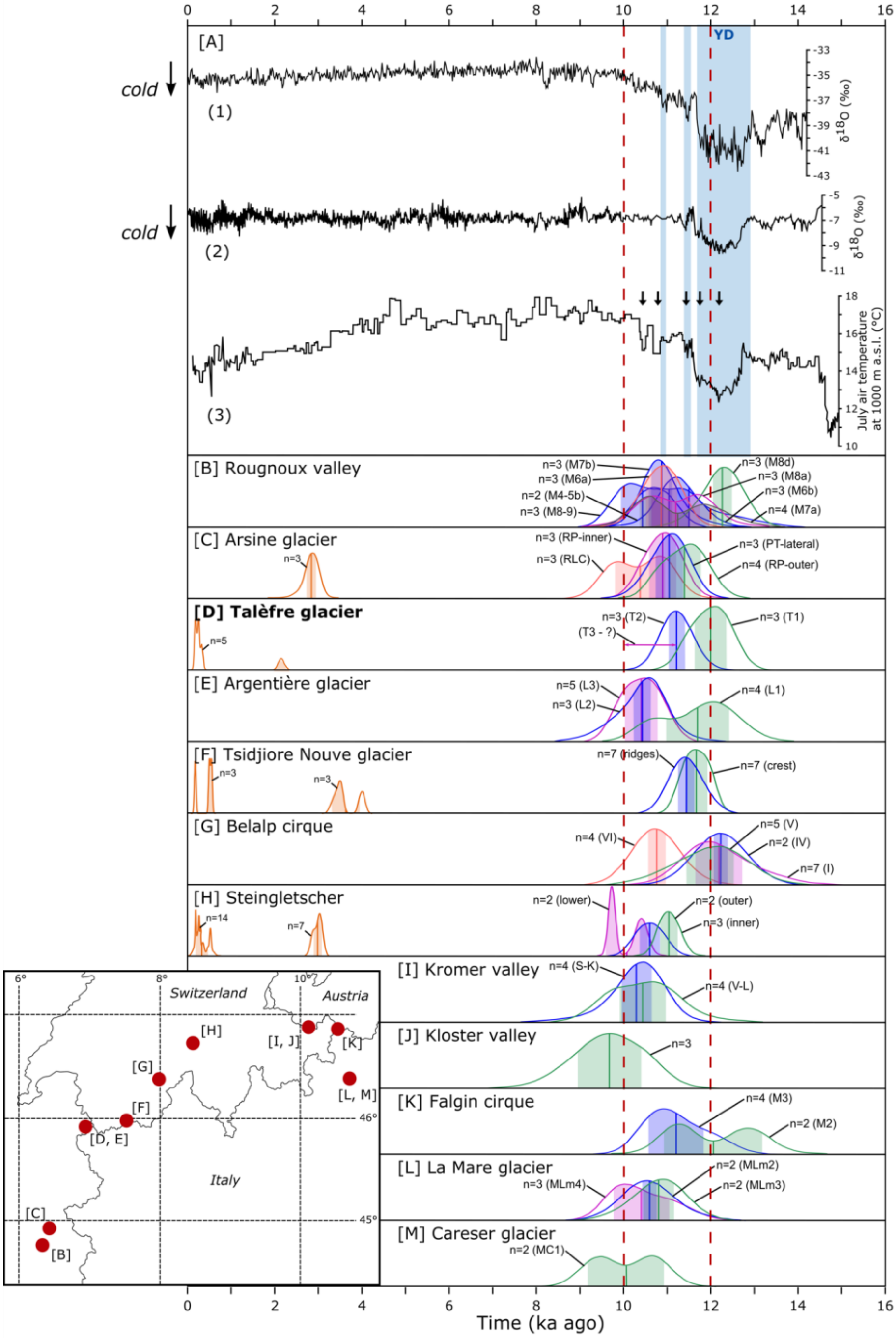

[A]
YD
cold
(1)
δ18O (‰)
cold
(2)
δ18O (‰)
(3)
July air temperature at 1000 m a.s.l. (°C)
[B] Rougnoux valley
n=3 (M7b)
n=3 (M6a)
n=2 (M4-5b)
n=3 (M8-9)
n=3 (M8d)
n=3 (M8a)
n=3 (M6b)
n=4 (M7a)
[C] Arsine glacier
n=3
n=3 (RP-inner)
n=3 (RLC)
n=3 (PT-lateral)
n=4 (RP-outer)
[D] Talèfre glacier
n=5
n=3 (T2)
(T3 - ?)
n=3 (T1)
[E] Argentière glacier
n=5 (L3)
n=3 (L2)
n=4 (L1)
[F] Tsidjiore Nouve glacier
n=3
n=3
n=7 (ridges)
n=7 (crest)
[G] Belalp cirque
n=4 (VI)
n=5 (V)
n=2 (IV)
n=7 (I)
[H] Steingletscher
n=14
n=7
n=2 (lower)
n=2 (outer)
n=3 (inner)
[I] Kromer valley
n=4 (S-K)
n=4 (V-L)
[J] Kloster valley
n=3
[K] Falgin cirque
n=4 (M3)
n=2 (M2)
[L] La Mare glacier
n=3 (MLm4)
n=2 (MLm2)
n=2 (MLm3)
[M] Careser glacier
n=2 (MC1)
Time (ka ago)
Switzerland
Austria
Italy
[H]
[I, J]
[K]
[G]
[L, M]
[F]
[D, E]
[C]
[B]
6°
8°
10°
46°
45°

Fig. 6~~Fig. 6~~ in comparison with the Talèfre glacier moraine ages.

Discussion

Oscillations of Talèfre glacier since the Younger Dryas

According to the exposure ages of the two bedrock samples, the "Jardin de Talèfre" deglaciation started at ~12.4 ka, i.e. during the YD period, if a continuous exposure scenario is assumed. Alternatively, the duration of ~12.4 ka could be composed of several exposure periods, e.g. a few hundred years of ice-free conditions during the warmer Bølling/Allerød (~14.7 – 12.9 ka; Lotter et al., 2000; Rasmussen et al., 2006) and subsequent burial by the re-advancing glacier at the beginning of the YD. However, the only slightly younger mean age of moraine T1 (12.0 ± 0.4 ka) implies that Jardin de Talèfre was deglaciated during the YD and the central rock islet has remained ice-free since that time. The mean ages of moraines T1 and T2 are stratigraphically consistent (12.0 ± 0.4 ka and 11.2 ± 0.2 ka) and coincide with the YD/EH transition. We propose that the T3 moraine was deposited during the EH, as its morphology is very similar to T1 and T2 moraines. This suggests that the glacier underwent at least three advances or stillstands after the beginning of its retreat ~12.4 ka ago until the EH.

Four out of the five ages acquired from moraine T4 ~~are dated~~ ~~between~~ span from 0.18 ± 0.02 ka to ~~and~~ 0.33 ± 0.03 ka, with a mean age of 0.25 ± 0.06 years. These results indicate that the moraine was last overtopped at the end of the LIA, when several closely-spaced advances occurred. One out of the five samples of T4 is ~~dated to~~significantly older, 2.12 ± 0.07 years (JDT-16-3). This older age can be either explained by isotope inheritance from a previous exposure duration or by accretion phases of this massive moraine that pre-dated the deposition of the LIA boulders. Such advances prior to the LIA have been reported for other glaciers in

Commenté [MLR11]: Un 'âge' ne peut pas être 'daté'…

Mis en forme : Barré

the French Alps: between ~3.5 ka and 0.7 ka at Mer de Glace (Le Roy et al., 2015) and ~2.1 ka at Argentière glacier (Le Roy, 2012) and in the Ecrins-Pelvoux massif (Le Roy et al., 2017). However, our data do not allow us to decide which of the two hypotheses is more likely.

Fig. 5 ~~visualizes~~ shows the large YD/EH and LIA extents of Talèfre glacier in comparison to that of 2008 C.E. During the YD/EH and the LIA, the glacier is still connected with the Mer de Glace, and the LIA extent is only slightly smaller than that of the YD/EH, while in 2008 C.E. the glacier size is significantly reduced.

We do not have any evidence of glacier advances between the EH and the Late Holocene, which is consistent with a warmer and dryer climate, and thus unfavorable for glacier growth in the Alps, during this period (Ivy-Ochs et al., 2009). Therefore, we assume that Talèfre glacier was smaller than its LIA extent during this period.

Comparison with other Alpine glacier chronologies

The YD/Holocene chronology of Talèfre glacier is very similar to the one recently established at the nearby Argentière glacier (Protin et al., 2019). A similar set of bedrock surfaces (~2450m a.s.l.) and five lateral moraines (~2400 - 2150m a.s.l.), dated by in situ cosmogenic ^{10}Be to between ~11.7 ka and ~10.4 ka, provide evidence of deglaciation at the end of the YD and at least five glacier re-advances or stillstands during the YD/EH transition. When comparing these two age sets (

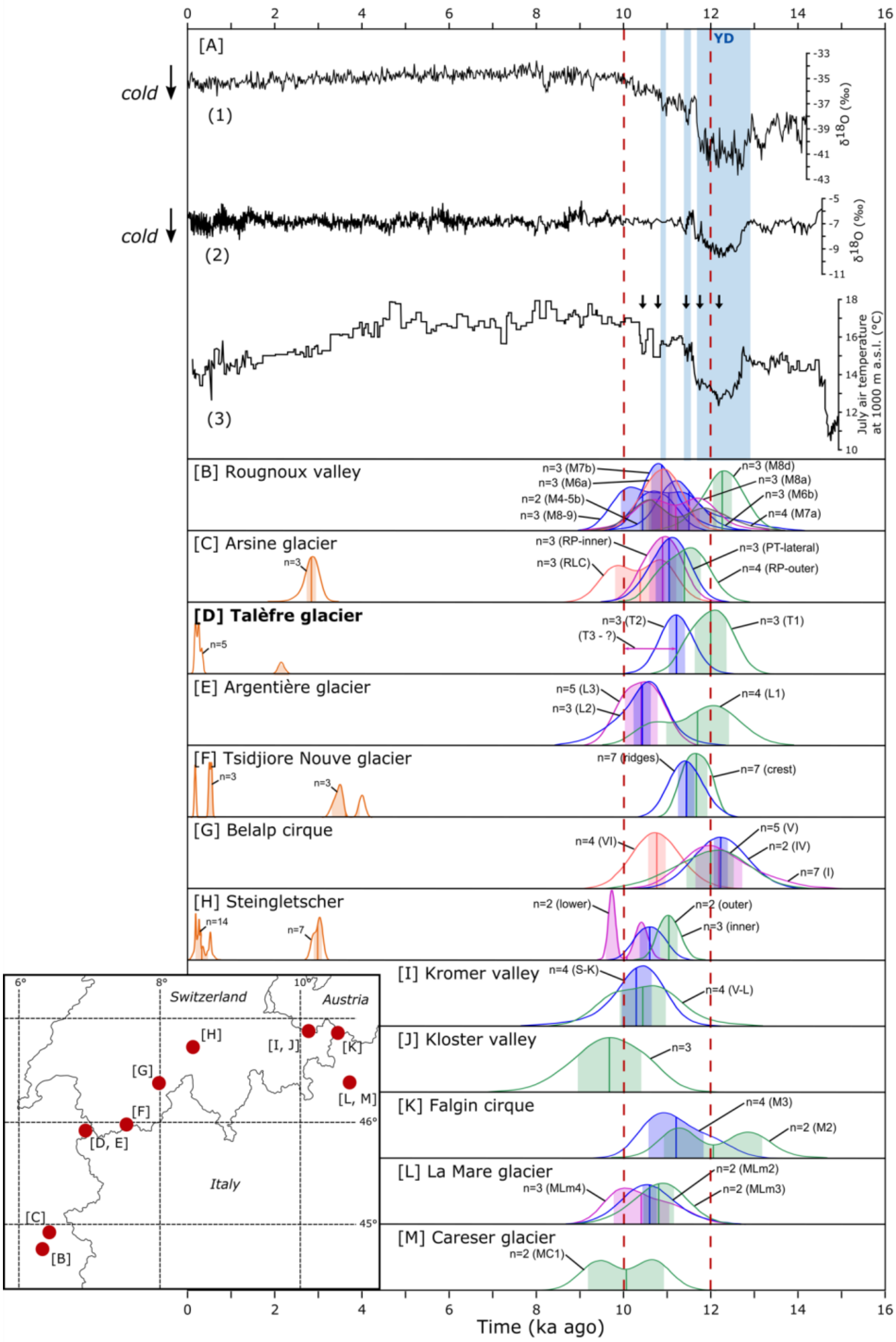

[A]
YD
cold
(1)
δ18O (‰)
cold
(2)
δ18O (‰)
(3)
July air temperature at 1000 m a.s.l. (°C)
[B] Rougnoux valley
n=3 (M7b)
n=3 (M6a)
n=2 (M4-5b)
n=3 (M8-9)
n=3 (M8d)
n=3 (M8a)
n=3 (M6b)
n=4 (M7a)
[C] Arsine glacier
n=3
n=3 (RP-inner)
n=3 (RLC)
n=3 (PT-lateral)
n=4 (RP-outer)
[D] Talèfre glacier
n=5
n=3 (T2)
(T3 - ?)
n=3 (T1)
[E] Argentière glacier
n=5 (L3)
n=3 (L2)
n=4 (L1)
[F] Tsidjiore Nouve glacier
n=3
n=3
n=7 (ridges)
n=7 (crest)
[G] Belalp cirque
n=4 (VI)
n=5 (V)
n=2 (IV)
n=7 (I)
[H] Steingletscher
n=14
n=7
n=2 (lower)
n=2 (outer)
n=3 (inner)
[I] Kromer valley
n=4 (S-K)
n=4 (V-L)
[J] Kloster valley
n=3
[K] Falgin cirque
n=4 (M3)
n=2 (M2)
[L] La Mare glacier
n=3 (MLm4)
n=2 (MLm2)
n=2 (MLm3)
[M] Careser glacier
n=2 (MC1)
Time (ka ago)
Switzerland
Austria
Italy
6°
8°
10°
46°
45°
[H]
[I, J]
[K]
[G]
[L, M]
[F]
[D, E]
[C]
[B]

Fig. 6Fig. 6 [D] and [E]), it appears that the ages of the two outermost moraines of both glaciers are undistinguishable within uncertainties, and that both glaciers oscillated several times during the YD/EH transition. In this comparison, it must be kept in mind that T3 moraine of Talèfre glacier could not be dated, butdated but seems to be only slightly younger than T1 and T2 moraines (section “Moraine and bedrock exposure ages”), and) and might therefore be similar to the innermost EH ridge of Argentière glacier dated to 10.4 ± 0.2 ka. These moraines of Talèfre and Argentière glaciers thus probably represent quasi-synchronous, successive glacier stillstands within the dynamic YD/EH retreat from their larger early-YD extents.

Moraines at multiple other locations across the Alps have previously been assigned to the YD/EH transition based on ^{10}Be dating. Eleven of them were selected here, based on their data quality (see section “Results”), together with our new Talèfre chronology for this regional compilation. They are geographically distributed across the European Alps (France, Switzerland, Italy and Austria), situated between longitudes ~6.5°E and 10°E and latitudes 45.5°N and 47°N (Fig. 6). All of these twelve moraine chronologies indicate deposition of at least one moraine between ~12 and ~10 ka ago, *i.e.* during the YD/EH transition (Fig. 6). Further, at most sites, there is evidence of deposition of multiple lateral and/or latero-frontal moraines during this period. Successive moraines are located quite close to each other and in proximity to the LIA moraines, suggesting only slightly smaller glacier extents during the LIA than during the YD/EH compared to today’s reduced glacier sizes like at Talèfre glacier (Fig. 5). The highest spatial spread is found at Arsine glacier displaying YD/EH frontal moraines that are located about 1 km downstream of the LIA moraines (Schimmelpfennig et al., 2019; Le Roy et al., in prep). At several other sites in the Alps, lateral YD/EH moraines exist within < 300m-distance from lateral LIA moraines (Hofmann et al., 2019; Moran et al., 2016; Schimmelpfennig et al., 2019, 2014, 2012).

Commenté [MOU12]: And/or Schimmelpfennig et al., 2019 (poster)

Thus, based on the consistency of the ^{10}Be cosmogenic exposure ages, we show here that millennial-scale synchronous glacier fluctuations occurred in the European Alps, and that glaciers oscillated multiple times at centennial or sub-centennial scale superposed on a general retreat trend during the 12-10 ka period. However, based on the available datasets it is not possible to temporally correlate specific moraines between sites or to give evidence of a decadal or centennial-scale synchroneity of glacier dynamics within the ∼12-10 ka period, because of (i) the analytical and geomorphic uncertainties related to the dating method; (ii) the probably incomplete preservation of the moraine records or no deposition of the moraine; (iii) undated ridges within the investigated moraine sequences at several sites.

For the sites where ELA depressions between the YD/EH transition and the LIA have been calculated using the Accumulation Area Ratio method with a ratio of 0.67 (Table S1), no significant correlations between moraine ages and ELA depressions are observed (Fig. S1). In fact, the large range of ELA depressions supports the findings by Boxleitner et al. (2019) that indicate ELA depressions should not be used to temporally correlate moraines from different valleys, as previously proposed by Maisch (1981). This reflects the fact that ELA variations of individual glaciers might be significantly influenced by local precipitation amounts and local glacier morphology, as well as the limitations of the AAR method (e.g. Boxleitner et al., 2019; Reitner et al., 2016).

Link of the Alpine glacier oscillations with regional climate

Analysis of the geographic characteristics of the 12 selected sites implies that their millennial synchroneity is independent of their altitude range (at present between 1500 and 3400 m a.s.l.), orientation (all directions) and size (0.3 to 14 km^2) (Fig. S1). In the absence of common topographic characteristics of the glaciers, the only process to explain the millennial-scale synchronous fluctuations of independent ice masses fluctuations across the European Alps is a regional climatic signal that prevailed over local factors. Therefore, we here compare the moraine chronologies with regional - and high-latitude - independent climate proxy records in an effort to elucidate the spatial reach of the climatic evolution underlying the quasi-simultaneous glacier oscillations across the European Alps within their dynamic retreat. Glaciers are sensitive to a variety of climatic factors, but the main driver for large-scale, long-term glacier fluctuations in the mid- and high latitudes is the impact of summer temperature variations (e.g. Oerlemans, 2005; Solomina et al., 2015) on which we therefore ~~focussed~~focus~~ed~~. In addition, over the last century, annual mass balance of Alpine glaciers have been shown to be mainly driven by summer melting (Huss et al., 2010). In the Alpine and pre-Alpine region, evidence of a temperature minimum in the middle of the YD and several distinct cold events during a general warming trend within the 12-10 ka period comes from various high-resolution paleorecords that reflect variations either in July air temperatures (based on chironomid-inferred records from lakes in eastern France and the northern and central Swiss Alps; Heiri et al., 2015 -

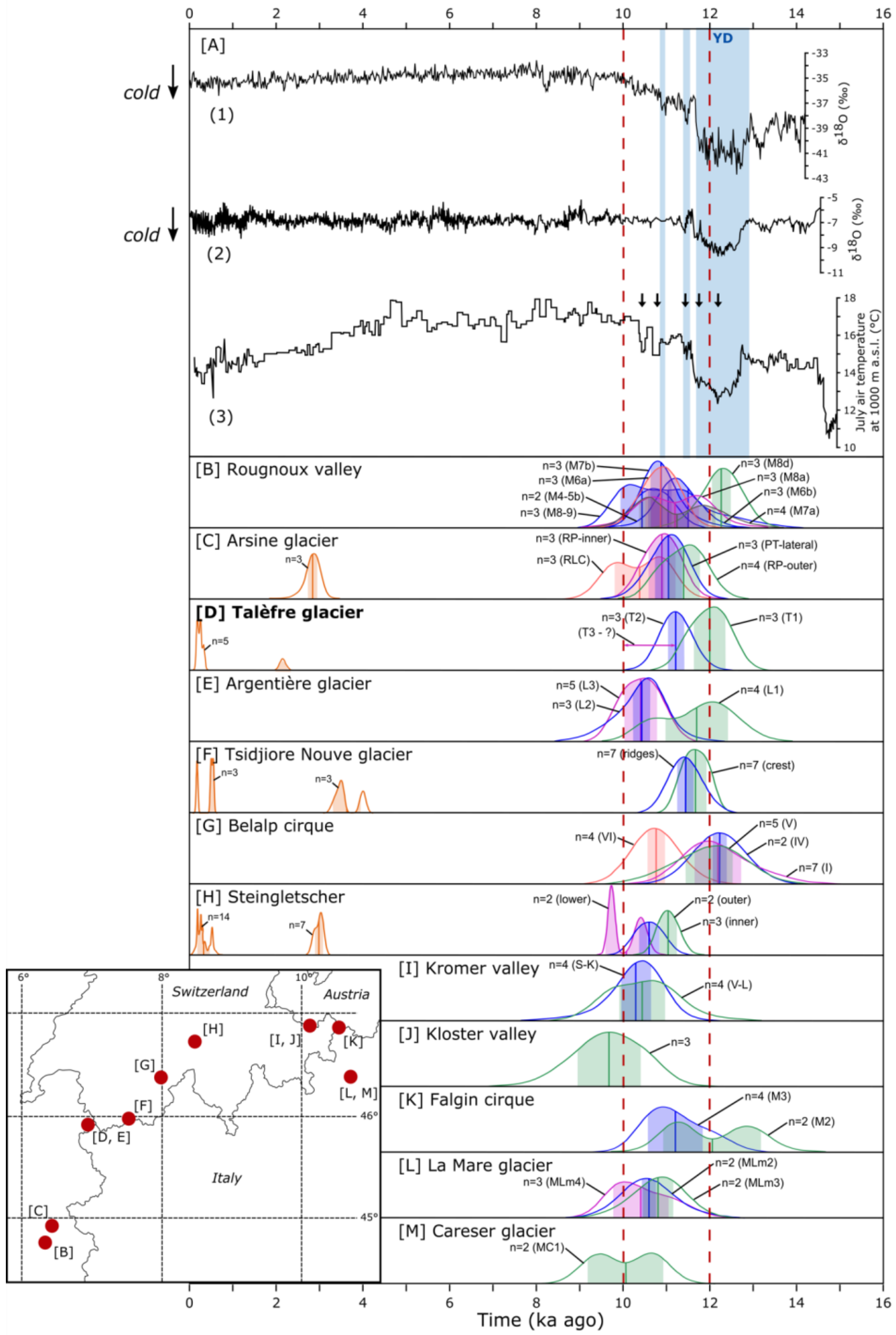

[A]
YD
cold
(1)
(2)
(3)
δ18O (‰)
July air temperature at 1000 m a.s.l. (°C)
[B] Rougnoux valley
n=3 (M7b)
n=3 (M6a)
n=2 (M4-5b)
n=3 (M8-9)
n=3 (M8d)
n=3 (M8a)
n=3 (M6b)
n=4 (M7a)
[C] Arsine glacier
n=3 (RP-inner)
n=3 (RLC)
n=3 (PT-lateral)
n=4 (RP-outer)
[D] Talèfre glacier
n=5
n=3 (T2)
(T3 - ?)
n=3 (T1)
[E] Argentière glacier
n=5 (L3)
n=3 (L2)
n=4 (L1)
[F] Tsidjiore Nouve glacier
n=3
n=7 (ridges)
n=7 (crest)
[G] Belalp cirque
n=4 (VI)
n=5 (V)
n=2 (IV)
n=7 (I)
[H] Steingletscher
n=14
n=7
n=2 (lower)
n=2 (outer)
n=3 (inner)
[I] Kromer valley
n=4 (S-K)
n=4 (V-L)
[J] Kloster valley
n=3
[K] Falgin cirque
n=4 (M3)
n=2 (M2)
[L] La Mare glacier
n=3 (MLm4)
n=2 (MLm2)
n=2 (MLm3)
[M] Careser glacier
n=2 (MC1)
Switzerland
Austria
Italy
6°
8°
10°
46°
45°
[H]
[I, J]
[K]
[G]
[L, M]
[F]
[D, E]
[C]
[B]
Time (ka ago)

Fig. 6~~Fig. 6~~ [A3]) or in mean annual temperatures, based on stable isotope measurements in stalagmites (Affolter et al., 2019 -

406 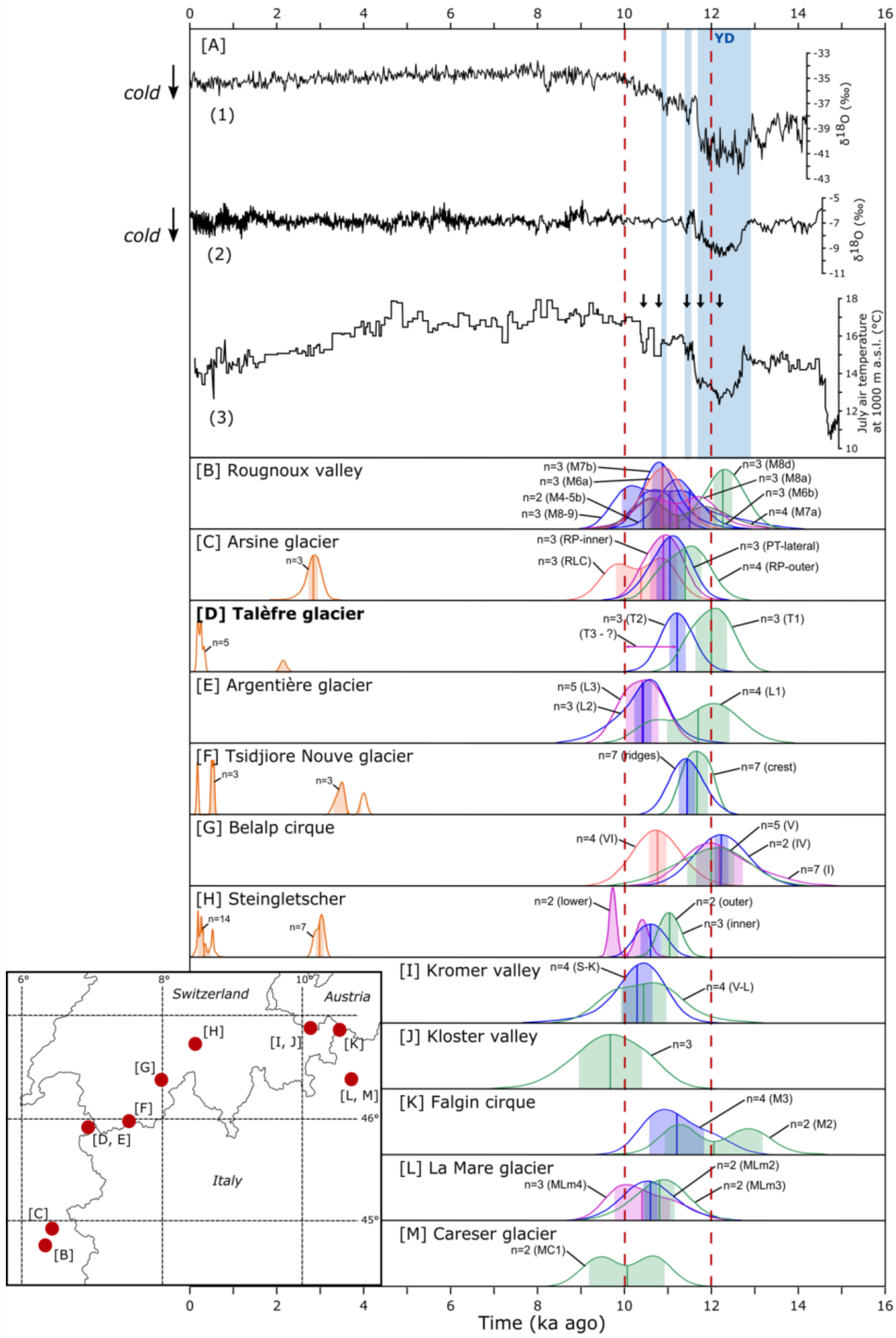
[A]
cold
(1)
(2)
(3)
YD
δ18O (‰)
July air temperature at 1000 m a.s.l. (°C)
[B] Rougnoux valley
[C] Arsine glacier
[D] Talèfre glacier
[E] Argentière glacier
[F] Tsidjiore Nouve glacier
[G] Belalp cirque
[H] Steingletscher
[I] Kromer valley
[J] Kloster valley
[K] Falgin cirque
[L] La Mare glacier
[M] Careser glacier
Switzerland
Austria
Italy
Time (ka ago)

Fig. 6~~Fig. 6~~ [A2]; Wurth et al., 2004) and biogenically precipitated carbonates in lake sediments (Schwander et al., 2000). These decadal to centennial cold peaks seem to have amplitudes in the order of ~0.5°C, i.e. similar to the multidecadal fluctuations that drove the succession of LIA moraines in the Alps (Oerlemans, 2005). Regional cold peaks could therefore be sufficient to lead to the YD/EH succession of glacial culminations or still-stands during the general deglaciation observed in the Alps. In this case, it is most likely that decadal to centennial glacier oscillations occurred quasi-simultaneously across the Alps.

Link of the Alpine glacier extents with seasonality

It is remarkable that several glaciers around 12 ka ago, i.e. at the end of the YD, were only slightly larger than during the EH. This is the case for Rougnoux valley, Arsine, Talèfre, Argentière, Tsidjiore Nouve, Belalp and Falgin Cirque glaciers, where the ages of the outermost moraine fall into the YD or their uncertainties overlap with it (green probability curves in

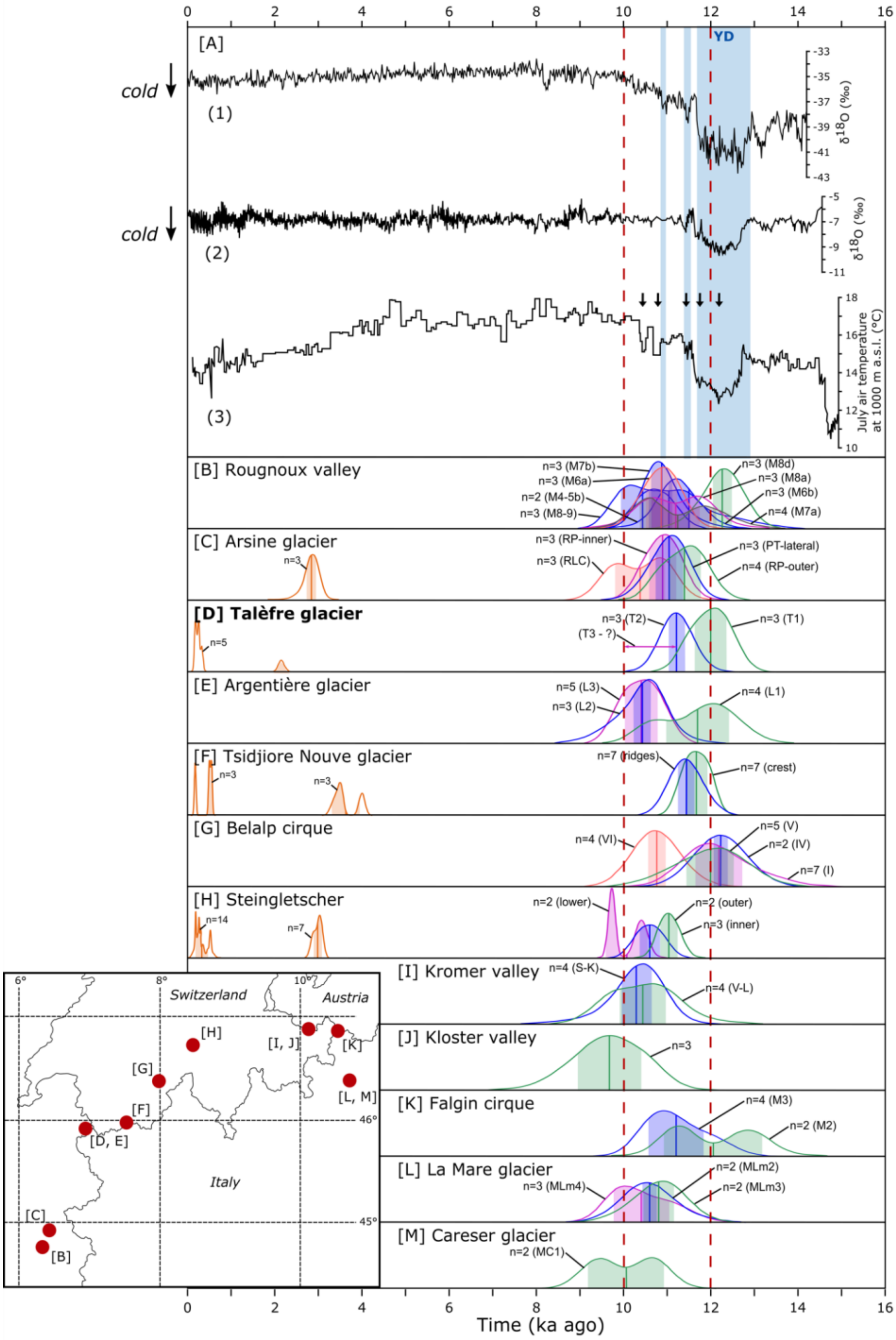

[A]
YD
cold
(1)
(2)
(3)
δ18O (‰)
July air temperature at 1000 m a.s.l. (°C)
[B] Rougnoux valley
n=3 (M7b)
n=3 (M6a)
n=2 (M4-5b)
n=3 (M8-9)
n=3 (M8d)
n=3 (M8a)
n=3 (M6b)
n=4 (M7a)
[C] Arsine glacier
n=3
n=3 (RP-inner)
n=3 (RLC)
n=3 (PT-lateral)
n=4 (RP-outer)
[D] Talèfre glacier
n=5
n=3 (T2)
(T3 - ?)
n=3 (T1)
[E] Argentière glacier
n=5 (L3)
n=3 (L2)
n=4 (L1)
[F] Tsidjiore Nouve glacier
n=3
n=3
n=7 (ridges)
n=7 (crest)
[G] Belalp cirque
n=4 (VI)
n=5 (V)
n=2 (IV)
n=7 (I)
[H] Steingletscher
n=14
n=7
n=2 (lower)
n=2 (outer)
n=3 (inner)
[I] Kromer valley
n=4 (S-K)
n=4 (V-L)
[J] Kloster valley
n=3
[K] Falgin cirque
n=4 (M3)
n=2 (M2)
[L] La Mare glacier
n=3 (MLm4)
n=2 (MLm2)
n=2 (MLm3)
[M] Careser glacier
n=2 (MC1)
Time (ka ago)
Switzerland
Austria
Italy
6°
8°
10°
46°
45°
[H]
[I, J]
[K]
[G]
[L, M]
[F]
[D, E]
[C]
[B]

Fig. 6~~Fig. 6~~) and the ages of the innermost moraine fall into the EH. This small difference between late YD and EH glacier extents seems inconsistent with the drastic YD temperature cooling and abrupt mean annual temperature increase that characterizes the boundary between these two periods (

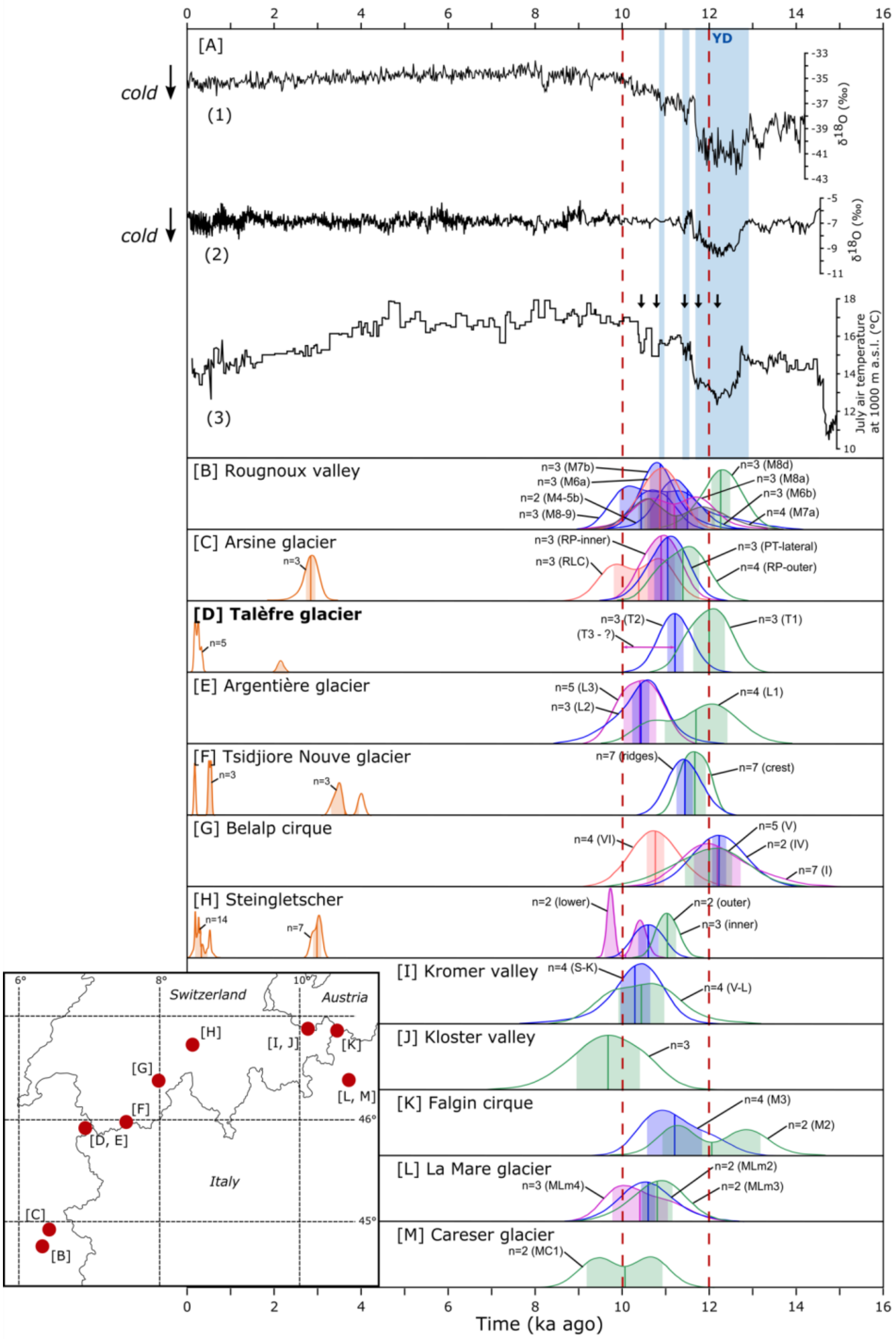

[A]
YD
cold
(1)
δ18O (‰)
cold
(2)
δ18O (‰)
(3)
July air temperature at 1000 m a.s.l. (°C)
[B] Rougnoux valley
n=3 (M7b)
n=3 (M6a)
n=2 (M4-5b)
n=3 (M8-9)
n=3 (M8d)
n=3 (M8a)
n=3 (M6b)
n=4 (M7a)
[C] Arsine glacier
n=3 (RP-inner)
n=3 (RLC)
n=3 (PT-lateral)
n=4 (RP-outer)
[D] Talèfre glacier
n=5
n=3 (T2)
(T3 - ?)
n=3 (T1)
[E] Argentière glacier
n=5 (L3)
n=3 (L2)
n=4 (L1)
[F] Tsidjiore Nouve glacier
n=3
n=7 (ridges)
n=7 (crest)
[G] Belalp cirque
n=4 (VI)
n=5 (V)
n=2 (IV)
n=7 (I)
[H] Steingletscher
n=14
n=7
n=2 (lower)
n=2 (outer)
n=3 (inner)
[I] Kromer valley
n=4 (S-K)
n=4 (V-L)
[J] Kloster valley
n=3
[K] Falgin cirque
n=4 (M3)
n=2 (M2)
[L] La Mare glacier
n=3 (MLm4)
n=2 (MLm2)
n=2 (MLm3)
[M] Careser glacier
n=2 (MC1)
Switzerland
Austria
Italy
Time (ka ago)

Fig. 6Fig. 6 [A]). A linear relationship between oxygen isotope record and temperature would suggest that the coldest YD temperatures of the Greenland sites were only slightly higher than those of the Last Glacial Maximum (e.g. Rasmussen et al., 2008) when Alpine glaciers reached until the Alpine foreland (Ivy-Ochs et al., 2008). Much larger glacier extents might therefore be expected during and at the end of the ~1 ka lasting YD, especially compared to the EH and LIA. In addition, the ^{10}Be bedrock ages from outboard of the oldest dated moraines of Talèfre and Argentière glaciers suggest that these glaciers have been retreating prior to the deposition of their respective late YD moraine. These results are in line with ^{10}Be-based glacier chronologies from Greenland, also providing evidence of ice mass downwasting throughout the YD, which lasted until the EH (Rainsley et al., 2018 and references therein).

The apparent mismatch between the glacier proxy records and the mean annual temperature climate proxies could be due to a difference in seasonality between the YD and the EH. This concept of seasonality was first proposed by Denton et al. (2005) to explain the discord between the drastic change of the mean annual temperature observed in Greenland ice cores and the slight snowline change of glaciers in Greenland and Europe during the YD and EH. The YD, as well as other abrupt climate changes, has been qualified as a winter phenomenon (Denton et al., 2005), meaning that the considerable annual temperature switches observed in paleoclimate records from Europe and Greenland are mainly due to changes in winter temperature, while summer temperature did only undergo minor changes (Buizert et al., 2014; Renssen and Isarin, 2001; Schenk et al., 2018).

In the Alpine region, a decrease of the seasonality between the YD and EH is supported by the difference of mean annual and summer warming estimated from the above-mentioned recent independent proxy studies (

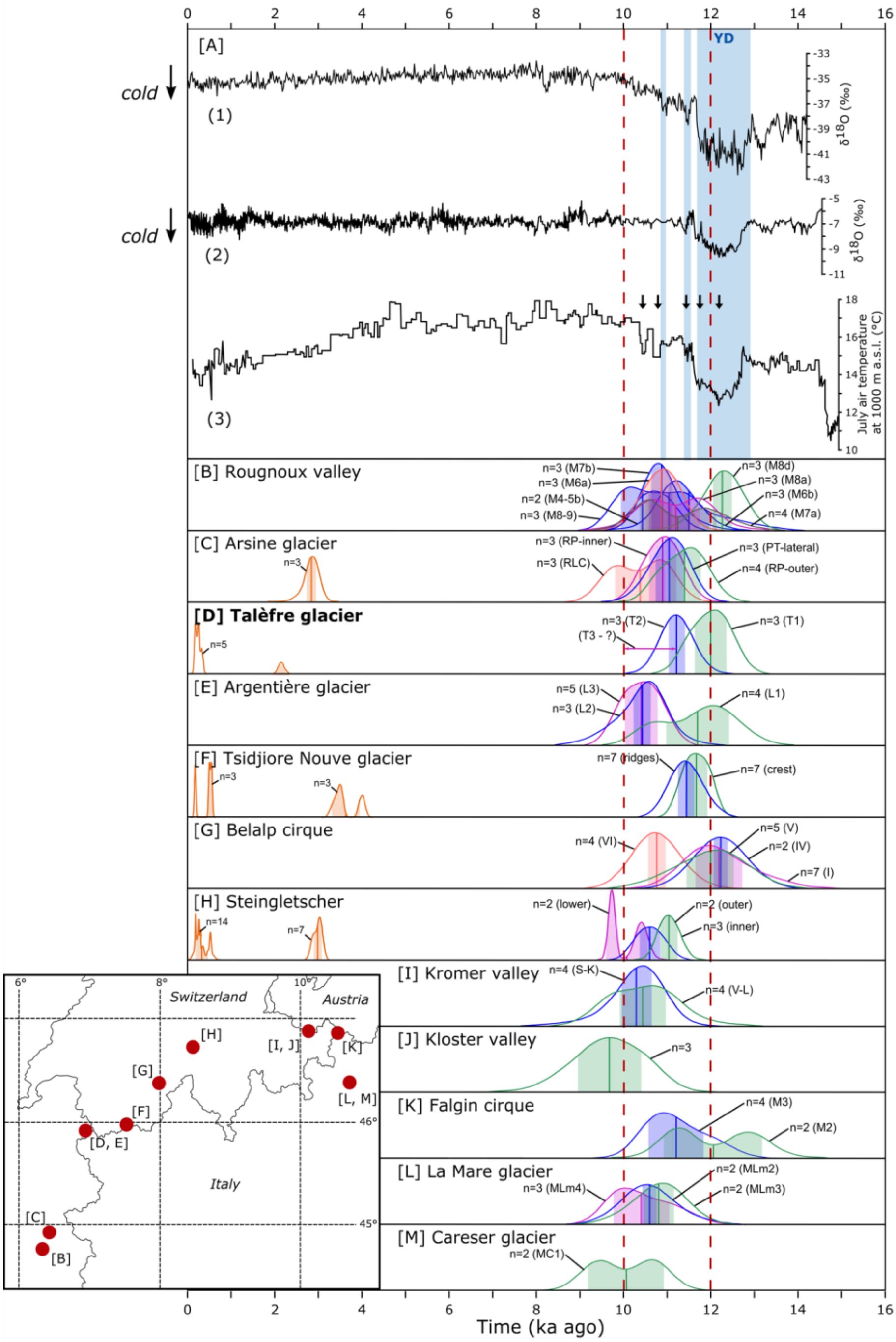
cold
(1)
cold
(2)
(3)
[A]
YD
δ18O (‰)
July air temperature at 1000 m a.s.l. (°C)
[B] Rougnoux valley
[C] Arsine glacier
[D] Talèfre glacier
[E] Argentière glacier
[F] Tsidjiore Nouve glacier
[G] Belalp cirque
[H] Steingletscher
[I] Kromer valley
[J] Kloster valley
[K] Falgin cirque
[L] La Mare glacier
[M] Careser glacier
Switzerland
Austria
Italy
Time (ka ago)

449

Fig. 6Fig. 6 [A2, 3]; Affolter et al., 2019; Heiri et al., 2015). The stable isotope measurements in speleothems suggest an increase of the mean annual temperature of ~5.4°C at the YD/EH transition (

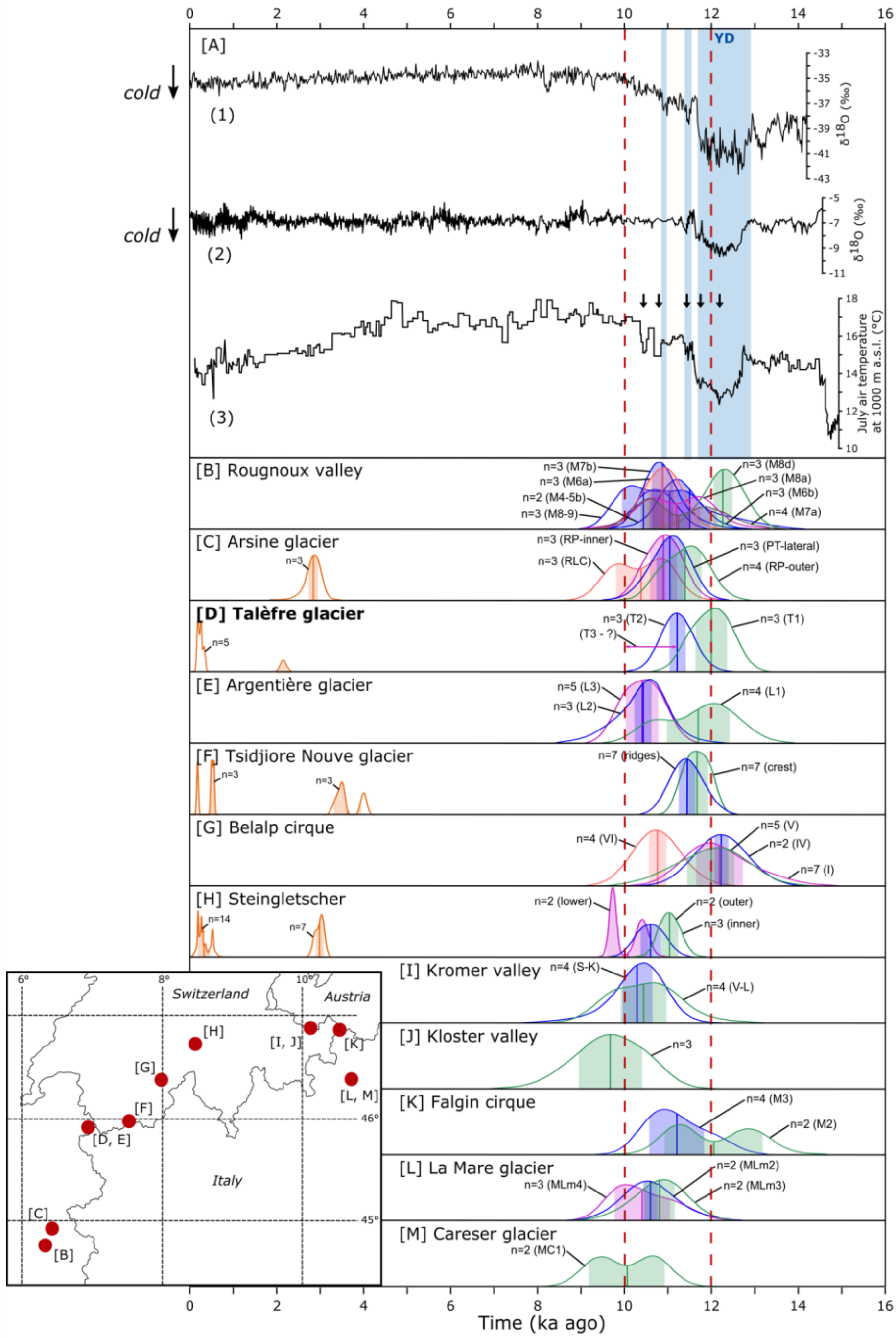

[A]
YD
cold
(1)
δ18O (‰)
cold
(2)
δ18O (‰)
(3)
July air temperature at 1000 m a.s.l. (°C)
[B] Rougnoux valley
n=3 (M7b)
n=3 (M6a)
n=2 (M4-5b)
n=3 (M8-9)
n=3 (M8d)
n=3 (M8a)
n=3 (M6b)
n=4 (M7a)
[C] Arsine glacier
n=3 (RP-inner)
n=3 (RLC)
n=3 (PT-lateral)
n=4 (RP-outer)
[D] Talèfre glacier
n=5
n=3 (T2)
(T3 - ?)
n=3 (T1)
[E] Argentière glacier
n=5 (L3)
n=3 (L2)
n=4 (L1)
[F] Tsidjiore Nouve glacier
n=3
n=7 (ridges)
n=7 (crest)
[G] Belalp cirque
n=4 (VI)
n=5 (V)
n=2 (IV)
n=7 (I)
[H] Steingletscher
n=14
n=7
n=2 (lower)
n=2 (outer)
n=3 (inner)
[I] Kromer valley
n=4 (S-K)
n=4 (V-L)
[J] Kloster valley
n=3
[K] Falgin cirque
n=4 (M3)
n=2 (M2)
[L] La Mare glacier
n=3 (MLm4)
n=2 (MLm2)
n=2 (MLm3)
[M] Careser glacier
n=2 (MC1)
Switzerland
Austria
Italy
6°
8°
10°
46°
45°
Time (ka ago)

Fig. 6~~Fig. 6~~ [A2]; Affolter et al., 2019), while a summer temperature increase of only ~2.7°C is inferred from the chironomid-based lake records (

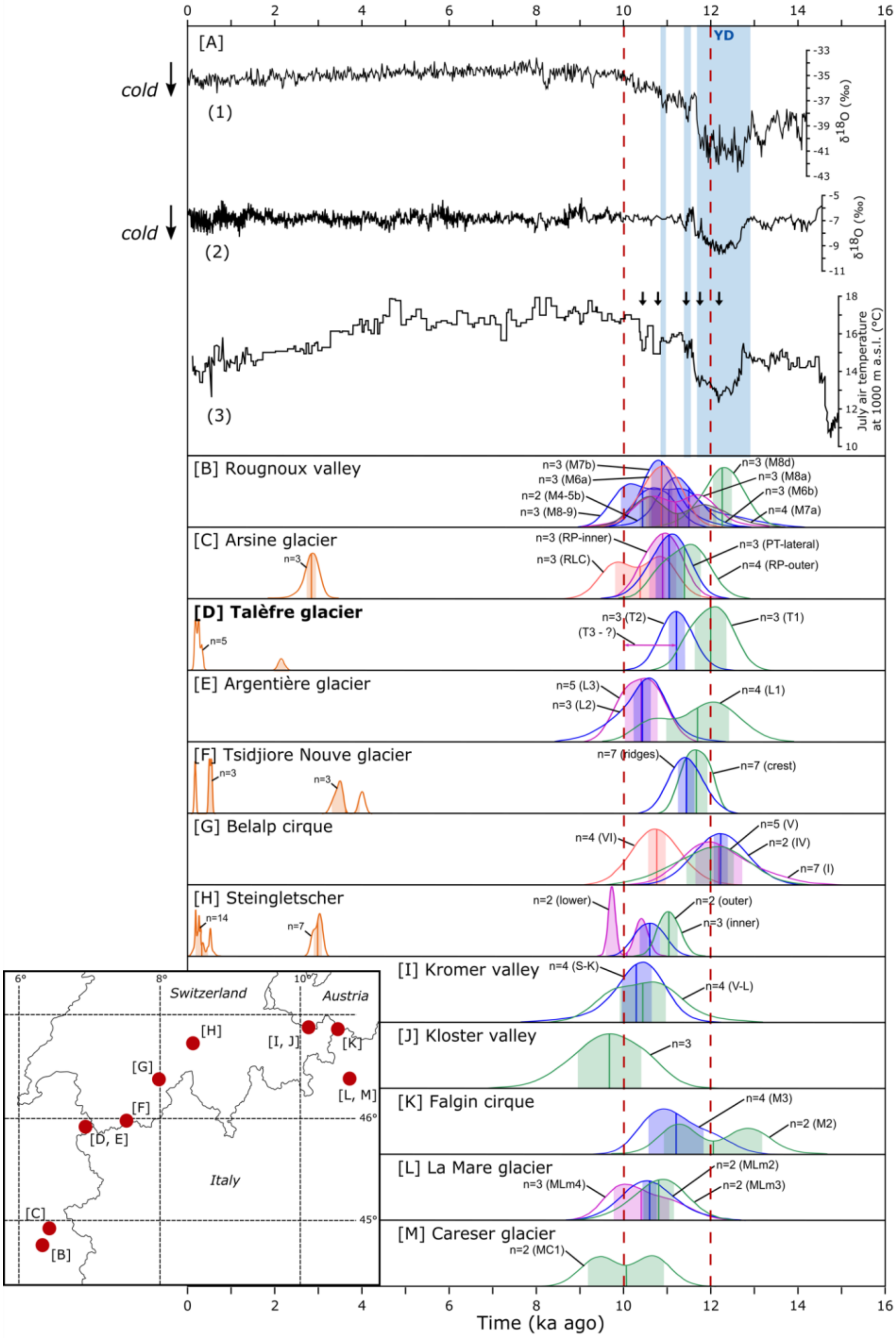

[A]
cold
(1)
(2)
(3)
YD
δ18O (‰)
July air temperature at 1000 m a.s.l. (°C)
[B] Rougnoux valley
[C] Arsine glacier
[D] Talèfre glacier
[E] Argentière glacier
[F] Tsidjiore Nouve glacier
[G] Belalp cirque
[H] Steingletscher
[I] Kromer valley
[J] Kloster valley
[K] Falgin cirque
[L] La Mare glacier
[M] Careser glacier
Switzerland
Austria
Italy
Time (ka ago)

456

Fig. 6~~Fig. 6~~ [A3]; Heiri et al., 2015). This difference between annual and summer temperature could be explained by a greater winter warming of more than 7°C if winter and summer periods are assumed of equal duration. Furthermore, while the mean temperature ~~increase~~increases in Greenland occurred in less than one hundred years (

Commenté [MOU13]: Moi, j'aurais laisser increase

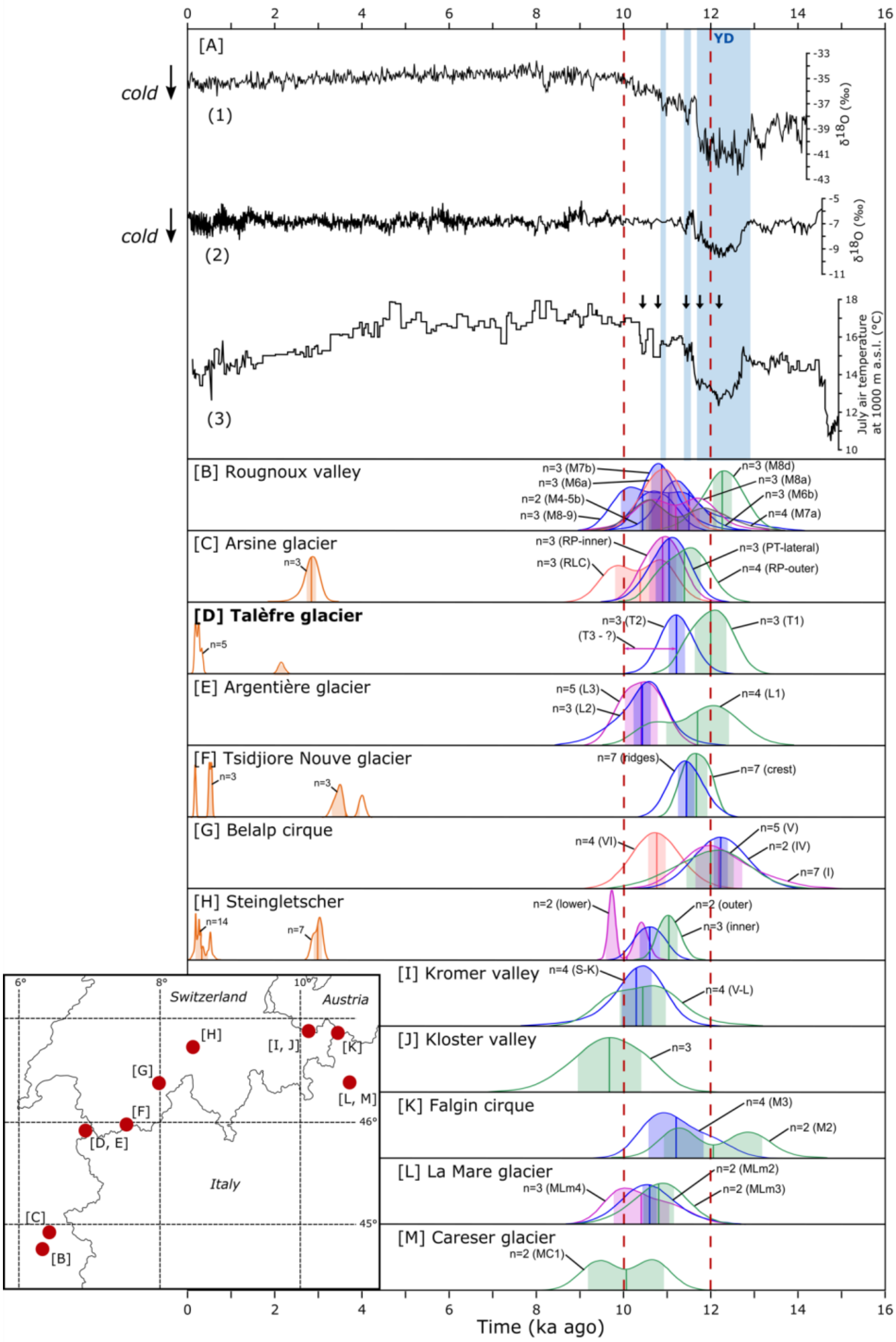

[A]
YD
cold
(1)
δ18O (‰)
cold
(2)
δ18O (‰)
(3)
July air temperature at 1000 m a.s.l. (°C)
[B] Rougnoux valley
n=3 (M7b)
n=3 (M6a)
n=2 (M4-5b)
n=3 (M8-9)
n=3 (M8d)
n=3 (M8a)
n=3 (M6b)
n=4 (M7a)
[C] Arsine glacier
n=3
n=3 (RP-inner)
n=3 (RLC)
n=3 (PT-lateral)
n=4 (RP-outer)
[D] Talèfre glacier
n=5
n=3 (T2)
(T3 - ?)
n=3 (T1)
[E] Argentière glacier
n=5 (L3)
n=3 (L2)
n=4 (L1)
[F] Tsidjiore Nouve glacier
n=3
n=3
n=7 (ridges)
n=7 (crest)
[G] Belalp cirque
n=4 (VI)
n=5 (V)
n=2 (IV)
n=7 (I)
[H] Steingletscher
n=14
n=7
n=2 (lower)
n=2 (outer)
n=3 (inner)
[I] Kromer valley
n=4 (S-K)
n=4 (V-L)
[J] Kloster valley
n=3
[K] Falgin cirque
n=4 (M3)
n=2 (M2)
[L] La Mare glacier
n=3 (MLm4)
n=2 (MLm2)
n=2 (MLm3)
[M] Careser glacier
n=2 (MC1)
Switzerland
Austria
Italy
[H]
[I, J]
[K]
[G]
[L, M]
[F]
[D, E]
[C]
[B]
6°
8°
10°
46°
45°
Time (ka ago)

Fig. 6Fig. 6 [A1]; Rasmussen et al., 2006), the European records indicate a more gradual warming distributed over several hundred years (

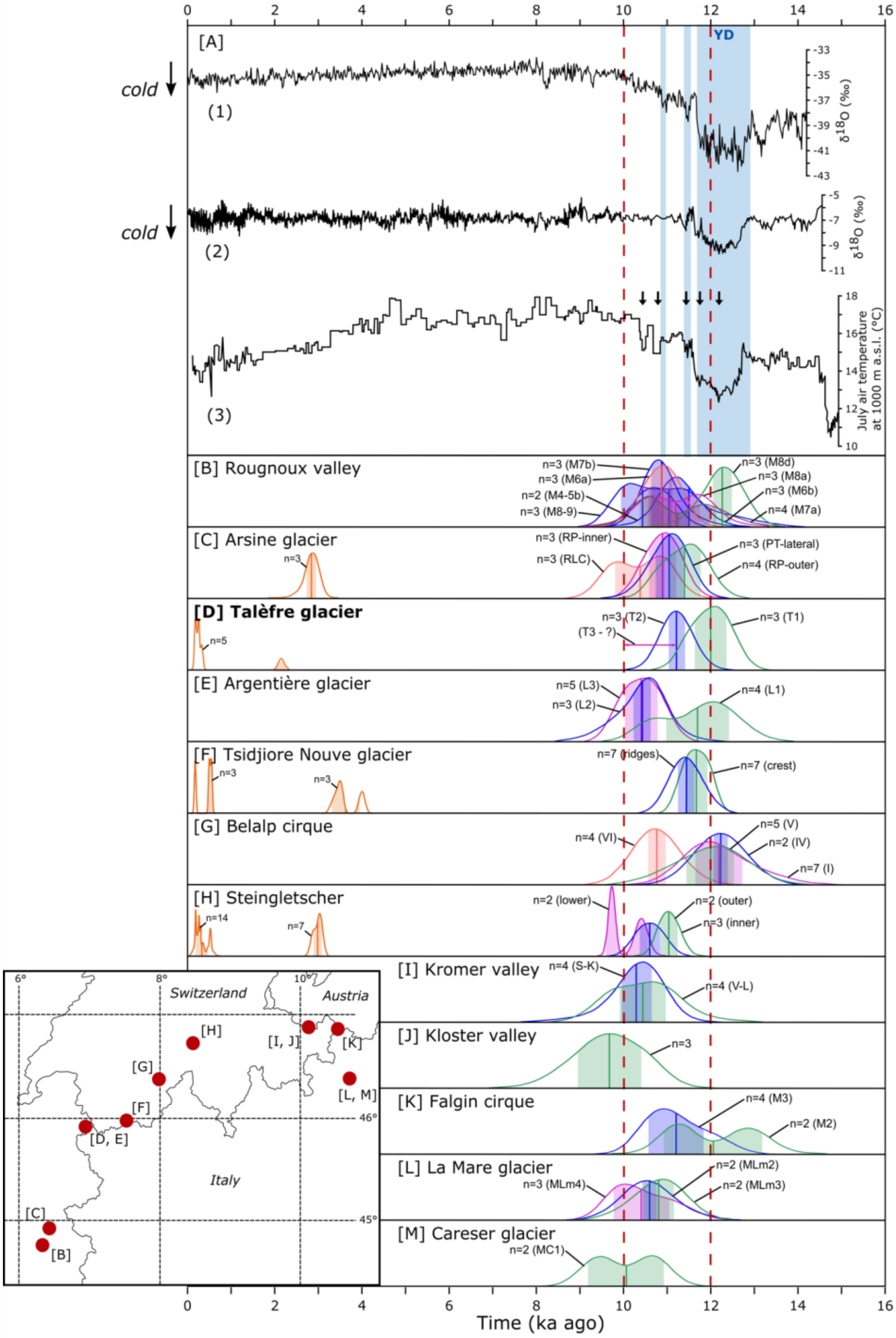
[A]
YD
cold
(1)
δ18O (‰)
cold
(2)
δ18O (‰)
(3)
July air temperature at 1000 m a.s.l. (°C)
[B] Rougnoux valley
[C] Arsine glacier
[D] Talèfre glacier
[E] Argentière glacier
[F] Tsidjiore Nouve glacier
[G] Belalp cirque
[H] Steingletscher
[I] Kromer valley
[J] Kloster valley
[K] Falgin cirque
[L] La Mare glacier
[M] Careser glacier
Switzerland
Austria
Italy
Time (ka ago)

464

Fig. 6Fig. 6 [A2, 3]). Our resultsobservations support this concept, i.e. relatively mild YD summer temperatures could explain why the glaciers in the Alps did not undergo a much more pronounced retreat at the YD/EH transition, but glaciers retreated gradually from their only slightly larger YD extents.

Link of the Alpine glacier oscillations with high latitude climate

The clear correlation of high-resolution proxy records from the Alps and the Alpine foreland (

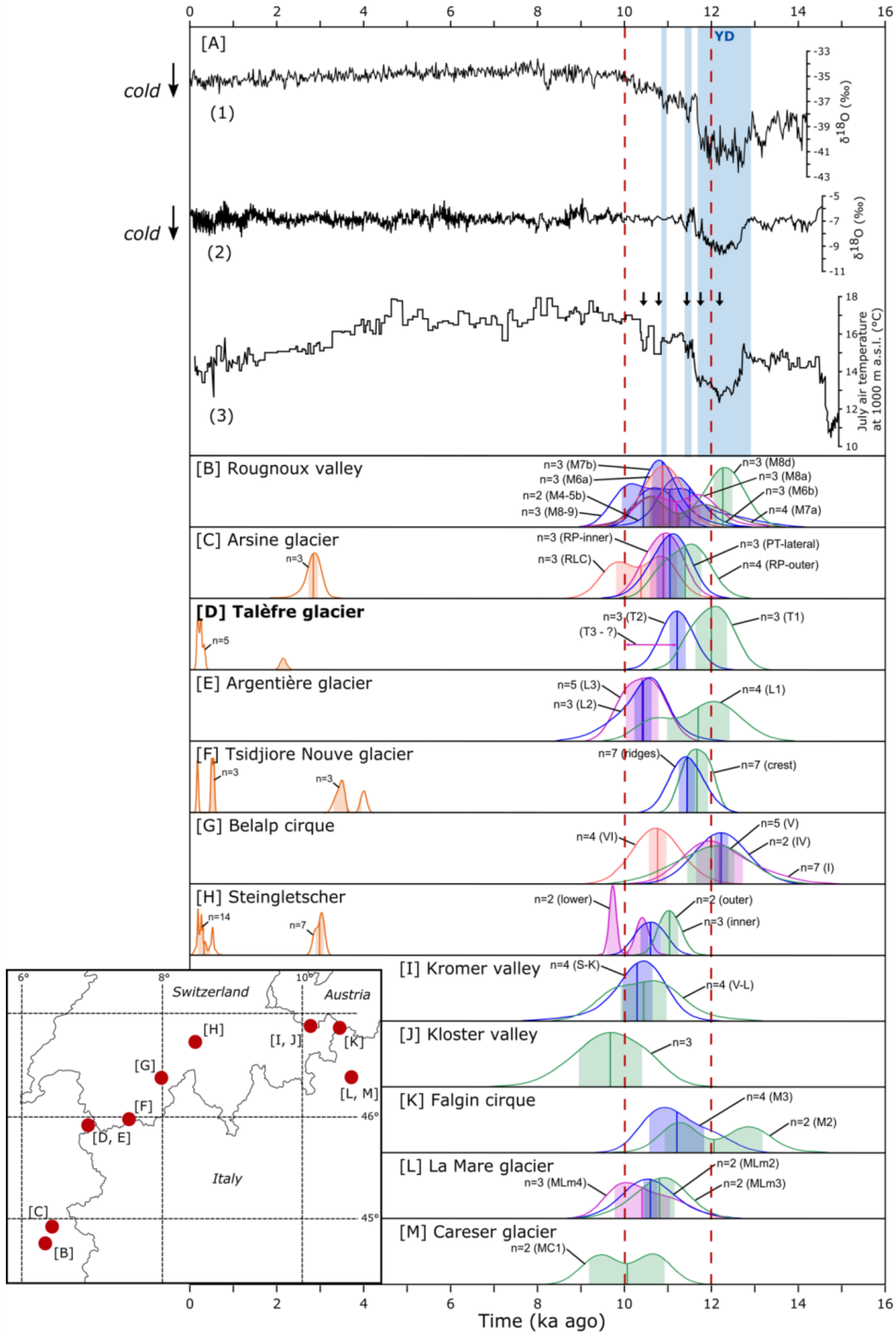

[A]
YD
cold
(1)
δ18O (‰)
cold
(2)
δ18O (‰)
(3)
July air temperature at 1000 m a.s.l. (°C)
[B] Rougnoux valley
n=3 (M7b)
n=3 (M6a)
n=2 (M4-5b)
n=3 (M8-9)
n=3 (M8d)
n=3 (M8a)
n=3 (M6b)
n=4 (M7a)
[C] Arsine glacier
n=3 (RP-inner)
n=3 (RLC)
n=3 (PT-lateral)
n=4 (RP-outer)
[D] Talèfre glacier
n=3 (T2)
(T3 - ?)
n=3 (T1)
n=5
[E] Argentière glacier
n=5 (L3)
n=3 (L2)
n=4 (L1)
[F] Tsidjiore Nouve glacier
n=7 (ridges)
n=7 (crest)
[G] Belalp cirque
n=4 (VI)
n=5 (V)
n=2 (IV)
n=7 (I)
[H] Steingletscher
n=2 (lower)
n=2 (outer)
n=3 (inner)
n=14
n=7
[I] Kromer valley
n=4 (S-K)
n=4 (V-L)
[J] Kloster valley
n=3
[K] Falgin cirque
n=4 (M3)
n=2 (M2)
[L] La Mare glacier
n=3 (MLm4)
n=2 (MLm2)
n=2 (MLm3)
[M] Careser glacier
n=2 (MC1)
Switzerland
Austria
Italy
Time (ka ago)

Fig. 6~~Fig. 6~~ [A2, 3]; Affolter et al., 2019; Heiri et al., 2015) with the pattern of oxygen isotope variations in Greenland ice cores (e.g. Rasmussen et al., 2006;

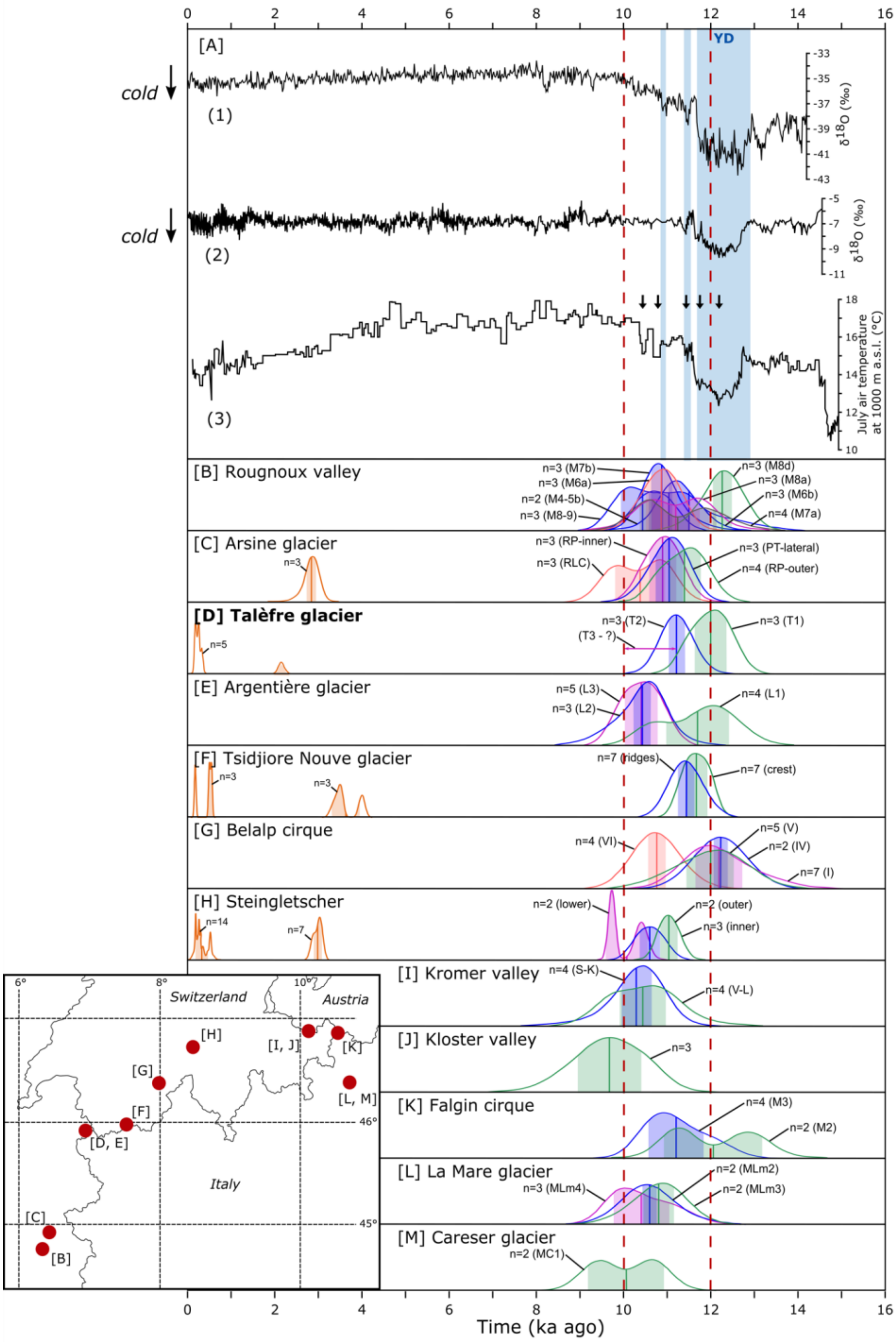

[A]
YD
cold
(1)
δ18O (‰)
cold
(2)
δ18O (‰)
(3)
July air temperature at 1000 m a.s.l. (°C)
[B] Rougnoux valley
[C] Arsine glacier
[D] Talèfre glacier
[E] Argentière glacier
[F] Tsidjiore Nouve glacier
[G] Belalp cirque
[H] Steingletscher
[I] Kromer valley
[J] Kloster valley
[K] Falgin cirque
[L] La Mare glacier
[M] Careser glacier
Switzerland
Austria
Italy
Time (ka ago)

475

Fig. 6~~Fig. 6~~ [A1]) strongly suggests a climatic link of the Alpine region with the northern high latitudes. In this context, a recent study by Young et al. (2020) provides evidence of a succession of re-advances or stillstands of~~ a~~ mountain glaciers, the Laurentide Ice Sheet and Greenland Ice Sheet in the Baffin Bay region at ∼11.8-11.6 ka, ~10.4 ka, ~9.3 ka. The striking similarity of these moraine-based chronologies from and near western Greenland with those from the European Alps provide further evidence of a teleconnection between both regions at that time and that the observed glacier fluctuations were due to a common climate evolution on extra-regional, maybe even hemispheric scale.

The question arises which large-scale climate mechanisms led to this teleconnection and the contrasted seasonality imprinted in the above-discussed summer temperature and mean annual temperature records. The abrupt onset of the YD cooling and the cold peaks of the Late YD and EH in the high latitudes are thought to have been triggered by freshwater input from the Laurentide Ice Sheet into the North Atlantic (Jennings et al., 2015) leading to a reduction of the Atlantic Meridional Ocean Circulation (AMOC) (Renssen et al., 2015). The related development of expanded wintertime sea ice in the North Atlantic shifted the westerlies south leading to wind-transported cool temperatures to Europe (Bakke et al., 2009; Brauer et al., 2008), and therefore to the Alps. During the second half of the YD, brief sea-ice breakups were led by incursions of the Atlantic circulation and were associated with a northwards migration of the polar front and westerly storm tracks (Bakke et al., 2009) until the system abruptly switched to the interglacial state at the onset of the Holocene (Rasmussen et al., 2006). The signature of these climatic mechanisms is markedly imprinted in the abrupt variations of the mean annual temperature proxy records, but to a lesser degree in the glacier mass balance fluctuations. Robust evidence of drastic glacier expansion in the Alps and the high latitudes in relation with the strong annual cooling observed in the first part of the YD is rare so far. Early to mid-YD moraines are preserved at a few sites in the Alps and at other sites in the North

Atlantic region (e.g. Belalp and Aletsch Glacier, Kelly et al., 2004; Schindelwig et al., 2012; Julier Pass, Ivy-Ochs, 2015; Alaska, Young et al., 2019; Norway, Wittmeier et al., 2020), but the corresponding glacier extents were relatively modest compared to significant annual temperature decrease. In addition, the deglaciation during the YD/EH transition was rather gradual and punctuated by closely-spaced short-lived re-advances or stillstands. This could be explained by several mechanisms. Sea ice expansion occurs predominantly in winter and might therefore not directly result in a summer temperature decrease. In addition, the drastic YD cooling recorded by the mean annual temperature proxies was enhanced by an increased strength of wind only during autumn, winter and spring, which transported cold air from the ice-covered North Atlantic region and led to cool and dry winters in Europe (Brauer et al., 2008). This phenomenon did not occur during summer due to atmospheric blocking of the cold westerlies over Fennoscandia leading to warm summers during the YD (Schenk et al., 2018). Therefore, and because snowfall was reduced during the dry winters of the cold periods, greater glacier expansion did not occur at many sites. Nevertheless, summers were very short, probably because winter sea ice expansion lasted for a long period of the year, leading to a reduced glacier melt season (Young et al., 2020). This might explain why glaciers responded with successive glacier advances or stillstands to these dynamic changes in seasonality both in high latitudes and Europe.

Conclusion

Our new chronology based on 14 ^{10}Be cosmogenic exposure ages on moraine and bedrock from the “Jardin de Talèfre” suggests that Talèfre glacier retreated from its YD position starting ~12.4 ka ago. This retreat was interrupted by several episodes of stillstands before a major retreat during the EH. No evidence of re-advances before the Late Holocene is preserved, with the most remarkable advance during the LIA, which was only slightly less extensive than the late YD and EH glacier extents at our high-elevation site. This behavior is very similar to that of the nearby Argentière glacier. The comparison of the YD/EH transition moraine chronology of Talèfre glacier with those of eleven other Alpine glaciers scattered throughout the Alps suggests a period of roughly synchronous glacial behavior across the Alps between 12 and 10 ka ago. Several glaciers deposited multiple moraines, which attest to regional-scale stillstands or re-advances during the deglaciation. Similarities with paleotemperature records from the Alpine region as well as with glacial culminations and temperature records from Greenland strongly suggest not only a regional-wide common climate driver, but also a teleconnection with the high latitudes, thus reinforcing the hypothesis postulated in earlier studies of a link between YD and EH Alpine glacier fluctuations and Greenland climate change. However, the relatively small amplitude of the YD glacier extents compared to the Holocene glacier extents is inconsistent with the large and abrupt temperature shifts imprinted in mean annual proxy records in both regions. We suggest that this inconsistency is due to a pronounced change in seasonality, with YD winters cold and dry and YD summers only slightly cooler than those of the EH. This seasonality difference controlled YD glacier extents and led to YD glaciers only slightly larger than during the EH.

Acknowledgements

This study is part of ANR 14-CE03-0006 *VIP Mont-Blanc*. We thank Laëtitia Léanni (CEREGE) for support during chemistry and Jean Hanley and Roseanne Schwartz (LDEO, Columbia University) for advices on sample chemistry and Joerg Schaefer (LDEO, Columbia University) for discussion. The ASTER AMS national facility (CEREGE) is supported by the INSU/CNRS, the ANR through the “projet thématiques d’excellence” program for the “Equipements d’excellence” ASTER-CEREGE action and IRD. An earlier version of this manuscript greatly benefitted from constructive comments by Benjamin Chandler. We thank

Marie Chenet and an anonymous reviewer whose relevant comments have helped to improve this manuscript.

Author contributions

JLM, IS, JFB and BP acquired the funding for the project leading to this publication. MP, JLM, JFB, BP and LM conducted the fieldwork. MP carried out the laboratory work. ASTER Team realized the AMS measurements. MP, IS, ~~and~~ JLM and MLR did the data analysis and prepared the original draft of the manuscript and all co-authors contributed the final draft of the manuscript.

Commenté [MLR14]: Comme il faut faire apparaitre la tache de tous les co-auteurs à cet endroit je suggère que tu me mettes là…

Data availability

The data that support the findings of this study are available from the corresponding author upon reasonable request.

References

Affolter, S., Häuselmann, A., Fleitmann, D., Edwards, R.L., Cheng, H., Leuenberger, M., 2019: Central Europe temperature constrained by speleothem fluid inclusion water isotopes over the past 14,000 years. *Science Advances* 5, eaav3809.

André, M., 2002: Rates of postglacial rock weathering on glacially scoured outcrops (abisko–riksgränsen area, 68°n): *Geografiska Annaler: Series A, Physical Geography* 84, 139–150.

Arnold, M., Merchel, S., Bourlès, D.L., Braucher, R., Benedetti, L., Finkel, R.C., Aumaître, G., Gottdang, A., Klein, M., 2010: The French accelerator mass spectrometry facility ASTER: Improved performance and developments. *Nuclear Instruments and Methods in Physics Research Section B: Beam Interactions with Materials and Atoms* 268, 1954–1959.

Bakke, J., Lie, Ø., Heegaard, E., Dokken, T., Haug, G.H., Birks, H.H., Dulski, P., Nilsen, T., 2009: Rapid oceanic and atmospheric changes during the Younger Dryas cold period. *Nature Geoscience* 2, 202–205.

Balco, G., 2017: Production rate calculations for cosmic-ray-muon-produced 10 Be and 26 Al benchmarked against geological calibration data. *Quaternary Geochronology* 39, 150-173.

Balco, G., Briner, J., Finkel, R.C., Rayburn, J.A., Ridge, J.C., Schaefer, J.M., 2009: Regional beryllium-10 production rate calibration for late-glacial northeastern North America. *Quaternary Geochronology* 4, 93–107.

Balco, G., Stone, J.O., Lifton, N.A., Dunai, T.J., 2008: A complete and easily accessible means of calculating surface exposure ages or erosion rates from 10Be and 26Al measurements. *Quaternary Geochronology* 3, 174–195.

Baroni, C., Casale, S., Salvatore, M.C., Ivy-Ochs, S., Christl, M., Carturan, L., Seppi, R., Carton, A., 2017: Double response of glaciers in the Upper Peio Valley (Rhaetian Alps, Italy) to the Younger Dryas climatic deterioration. *Boreas* 46, 783–798.

Borchers, B., Marrero, S., Balco, G., Caffee, M., Goehring, B., Lifton, N., Nishiizumi, K., Phillips, F., Schaefer, J., Stone, J., 2016: Geological calibration of spallation production rates in the CRONUS-Earth project. *Quaternary Geochronology* 31, 188–198.

Boxleitner, M., Ivy-Ochs, S., Egli, M., Brandova, D., Christl, M., Maisch, M., 2019: Lateglacial and Early Holocene glacier stages - New dating evidence from the Meiental in central Switzerland. *Geomorphology* 340, 15-31.

Braucher, R., Guillou, V., Bourlès, D.L., Arnold, M., Aumaître, G., Keddadouche, K., Nottoli, E., 2015: Preparation of ASTER in-house 10Be/9Be standard solutions. *Nuclear Instruments and Methods in Physics Research Section B: Beam Interactions with Materials and Atoms* 361, 335–340.

Brauer, A., Haug, G.H., Dulski, P., Sigman, D.M., Negendank, J.F.W., 2008: An abrupt wind shift in western Europe at the onset of the Younger Dryas cold period. *Nature Geoscience* 1, 520–523.

Braumann, S.M., Schaefer, J.M., Neuhuber, S.M., Reitner, J.M., Lüthgens, C., Fiebig, M., 2020: Holocene glacier change in the Silvretta Massif (Austrian Alps) constrained by a new 10Be chronology, historical records and modern observations. *Quaternary Science Reviews* 245, 106493.

Buizert, C., Gkinis, V., Severinghaus, J.P., He, F., Lecavalier, B.S., Kindler, P., Leuenberger, M., Carlson, A.E., Vinther, B., Masson-Delmotte, V., White, J.W.C., Liu, Z., Otto-Bliesner, B., Brook, E.J., 2014: Greenland temperature response to climate forcing during the last deglaciation. *Science* 345, 1177–1180.

Bussy, F., Hernandez, J., Raumer, J.V., 2000. Bimodal magmatism as a consequence of the post-collisional readjustment of the thickened Variscan continental lithosphere (Aiguilles Rouges-Mont Blanc Massifs, Western Alps). *Earth and Environmental Science Transactions of The Royal Society of Edinburgh* 91, 221–233.

Chenet, M., Brunstein, D., Jomelli, V., Roussel, E., Rinterknecht, V., Mokadem, F., Biette, M., Robert, V., Léanni, L., 2016: 10Be cosmic-ray exposure dating of moraines and rock avalanches in the Upper Romanche valley (French Alps): Evidence of two glacial advances during the Late Glacial/Holocene transition. *Quaternary Science Reviews* 148, 209–221.

Chmeleff, J., von Blanckenburg, F., Kossert, K., Jakob, D., 2010: Determination of the 10Be half-life by multicollector ICP-MS and liquid scintillation counting. *Nuclear Instruments and Methods in Physics Research Section B: Beam Interactions with Materials and Atoms* 268, 192–199.

Claude, A., Ivy-Ochs, S., Kober, F., Antognini, M., Salcher, B., Kubik, P.W., 2014: The Chironico landslide (Valle Leventina, southern Swiss Alps): age and evolution. *Swiss Journal of Geosciences* 107, 273–291.

Cossart, E., Fort, M., Bourlès, D., Braucher, R., Perrier, R., Siame, L., 2012: Deglaciation pattern during the Lateglacial/Holocene transition in the southern French Alps. Chronological data and geographical reconstruction from the Clarée Valley (upper Durance catchment, southeastern France). *Palaeogeography, Palaeoclimatology, Palaeoecology* 315–316, 109–123.

de Decker Heftler, S., 2002: Photographier le Mont Blanc, Guerin. ed.

Denton, G., Alley, R., Comer, G., Broecker, W., 2005: The role of seasonality in abrupt climate change. *Quaternary Science Reviews* 24, 1159–1182.

Fischer, M., Huss, M., Barboux, C., Hoelzle, M., 2014: The New Swiss Glacier Inventory SGI2010: Relevance of Using High-Resolution Source Data in Areas Dominated by Very Small Glaciers. *Arctic, Antarctic, and Alpine Research* 46, 933–945.

Gardent, M., 2014: Inventaire et retrait des glaciers dans les alpes françaises depuis la fin du Petit Age Glaciaire. (PhD thesis) Université de Grenoble.

Gardent, M., Rabatel, A., Dedieu, J.-P., Deline, P., 2014: Multitemporal glacier inventory of the French Alps from the late 1960s to the late 2000s. *Global and Planetary Change Glob. Planet. Change* 120, 24–37

Heiri, O., Ilyashuk, B., Millet, L., Samartin, S., Lotter, A.F., 2015: Stacking of discontinuous regional palaeoclimate records: Chironomid-based summer temperatures from the Alpine region. *The Holocene* 25, 137–149.

Hofmann, F.M., 2018: Glacial history of the upper Drac Blanc catchment (Écrins massif, French Alps). *E&G Quaternary Science Journal* 67, 37–40.

Hofmann, F.M., Alexanderson, H., Schoeneich, P., Mertes, J.R., Léanni, L., Aster Team (Georges Aumaître, Didier L. Bourlès, Karim Keddadouche), 2019: Post-Last Glacial Maximum glacier fluctuations in the southern Écrins massif (westernmost Alps): insights from 10Be cosmic ray exposure dating. *Boreas* 48, 1019-1041.

Huss, M., Hock, R., Bauder, A., Funk, M., 2010: 100-year mass changes in the Swiss Alps linked to the Atlantic Multidecadal Oscillation. *Geophysical Research Letters* 37, https://doi.org/10.1029/2010GL042616.

Ivy-Ochs, S., 2015: Glacier variations in the European Alps at the end of the last glaciation. *Cuadernos de Investigación Geográfica* 41, 295-315.

Ivy-Ochs, S., Kerschner, H., Maisch, M., Christl, M., Kubik, P.W., Schlüchter, C., 2009: Latest Pleistocene and Holocene glacier variations in the European Alps. *Quaternary Science Reviews* 28, 2137–2149.

Ivy-Ochs, S., Kerschner, H., Reuther, A., Maisch, M., Sailer, R., Schaefer, J., Kubik, P.W., Synal, H.-A., Schluechter, C., 2006: The timing of glacier advances in the northern European Alps based on surface exposure dating with cosmogenic 10Be, 26Al, 36Cl, and 21Ne. *In Situ-Produced Cosmogenic Nuclides and Quantification of Geological Processes*, Ana María Alonso-Zarza, Lawrence H. Tanner.

Ivy-Ochs, S., Kerschner, H., Reuther, A., Preusser, F., Heine, K., Maisch, M., Kubik, P.W., Schlüchter, C., 2008: Chronology of the last glacial cycle in the European Alps. *Journal of Quaternary Science* 23, 559–573.

Jennings, A., Andrews, J., Pearce, C., Wilson, L., Ólfasdótttir, S., 2015: Detrital carbonate peaks on the Labrador shelf, a 13–7ka template for freshwater forcing from the Hudson Strait outlet of the Laurentide Ice Sheet into the subpolar gyre. *Quaternary Science Reviews* 107, 62–80.

Joly, D., Berger, A., Buoncristiani, J.-F., Champagne, O., Pergaud, J., Richard, Y., Soare, P., Pohl, B., 2018: Geomatic downscaling of temperatures in the Mont Blanc massif: A NEW STATISTICAL DOWNSCALING APPROACH. *International Journal of Climatology* 38, 1846–1863.

Jordan, D., 2010: Le Jardin de Talèfre dans le massif du Mont-Blanc à Chamonix - Réévaluation et contribution à sa connaissance botanique. Monde Plantes 501.

Kelly, M.A., Kubik, P.W., Von Blanckenburg, F., SchlÜchter, C., 2004: Surface exposure dating of the Great Aletsch Glacier Egesen moraine system, western Swiss Alps, using the cosmogenic nuclide 10Be. *Journal of Quaternary Science* 19, 431–441.

Kerschner, H., Hertl, A., Gross, G., Ivy-Ochs, S., Kubik, P.W., 2006: Surface exposure dating of moraines in the Kromer valley (Silvretta Mountains, Austria)-evidence for glacial response to the 8.2 ka event in the Eastern Alps? *The Holocene* 16, 7–15.

Kobashi, T., Severinghaus, J.P., Barnola, J.-M., 2008: 4±1.5 °C abrupt warming 11,270 yr ago identified from trapped air in Greenland ice. *Earth and Planetary Science Letters* 268, 397–407.

Korschinek, G., Bergmaier, A., Faestermann, T., Gerstmann, U.C., Knie, K., Rugel, G., Wallner, A., Dillmann, I., Dollinger, G., von Gostomski, Ch.L., Kossert, K., Maiti, M., Poutivtsev, M., Remmert, A., 2010: A new value for the half-life of 10Be by Heavy-Ion Elastic Recoil Detection and liquid scintillation counting. *Nuclear Instruments and Methods in Physics Research Section B: Beam Interactions with Materials and Atoms* 268, 187–191.

Le Roy, M., 2012: Reconstitution des fluctuations glaciaires Holocènes dans les Alpes occidentales : apports de la dendrochronologie et de la datation par isotopes cosmogéniques produits in situ (PhD thesis). Université Grenoble Alpes.

Le Roy, M., Deline, P., Carcaillet, J., Schimmelpfennig, I., Ermini, M., 2017: 10Be exposure dating of the timing of Neoglacial glacier advances in the Ecrins-Pelvoux massif, southern French Alps. *Quaternary Science Reviews* 178, 118–138.

Le Roy, M., Nicolussi, K., Deline, P., Astrade, L., Edouard, J.-L., Miramont, C., Arnaud, F., 2015: Calendar-dated glacier variations in the western European Alps during the Neoglacial: the Mer de Glace record, Mont Blanc massif. *Quaternary Science Reviews* 108, 1–22.

Lotter, A.F., Birks, H.J.B., Eicher, U., Hofmann, W., Schwander, J., Wick, L., 2000: Younger Dryas and Allerød summer temperatures at Gerzensee (Switzerland) inferred from fossil pollen and cladoceran assemblages. *Palaeogeography, Palaeoclimatology, Palaeoecology* 159, 349–361.

Maisch, M., 1981: Glazialmorphologische und gletschergeschichtliche Untersuchungen im Gebiet zwischen Landwasser- und Albulatal (Kt. Graubünden, Schweiz).

Marsicek, J., Shuman, B.N., Bartlein, P.J., Shafer, S.L., Brewer, S., 2018: Reconciling divergent trends and millennial variations in Holocene temperatures. *Nature* 554, 92–96.

Martin, L.C.P., Blard, P.-H., Balco, G., Lavé, J., Delunel, R., Lifton, N., Laurent, V., 2017: The CREp program and the ICE-D production rate calibration database: A fully parameterizable and updated online tool to compute cosmic-ray exposure ages. *Quaternary Geochronology* 38, 25–49.

Merchel, S., Arnold, M., Aumaître, G., Benedetti, L., Bourlès, D.L., Braucher, R., Alfimov, V., Freeman, S.P.H.T., Steier, P., Wallner, A., 2008: Towards more precise 10Be and 36Cl data from measurements at the 10−14 level: Influence of sample preparation. *Nuclear Instruments and Methods in Physics Research Section B: Beam Interactions with Materials and Atoms* 266, 4921–4926.

Moran, A.P., Ivy-Ochs, S., Schuh, M., Christl, M., Kerschner, H., 2016a: Evidence of central Alpine glacier advances during the Younger Dryas–early Holocene transition period. *Boreas* 45, 398–410.

Moran, A.P., Kerschner, H., Ochs, S.I., 2016b: Redating the moraines in the Kromer Valley (Silvretta Mountains)–New evidence for an early Holocene glacier advance. *The Holocene* 26, 655–664.

Oerlemans, J., 2005: Extracting a Climate Signal from 169 Glacier Records. *Science* 308, 675–677.

Protin, M., Schimmelpfennig, I., Mugnier, J.-L., Ravanel, L., Le Roy, M., Deline, P., Favier, V., Buoncristiani, J.-F., Aumaître, G., Bourlès, D.L., Keddadouche, K., 2019 : Climatic reconstruction for the Younger Dryas/Early Holocene transition and the Little Ice Age based on paleo-extents of Argentière glacier (French Alps). *Quaternary Science Reviews* 221, 105863.

Prud'homme, C., Vassallo, R., Crouzet, C., Carcaillet, J., Mugnier, J.-L., Cortés-Aranda, J., 2020: Paired 10Be sampling of polished bedrock and erratic boulders to improve dating of glacial landforms: an example from the Western Alps. *Earth Surface Processes and Landforms* 45, 1168–1180.

Putnam, A.E., Bromley, G.R.M., Rademaker, K., Schaefer, J.M., 2019: In situ 10Be production-rate calibration from a 14C-dated late-glacial moraine belt in Rannoch Moor, central Scottish Highlands. *Quaternary Geochronology* 50, 109–125.

Rabatel, A., Letréguilly, A., Dedieu, J.-P., Eckert, N., 2013: Changes in glacier equilibrium-line altitude in the western Alps from 1984 to 2010: evaluation by remote sensing and modeling of the morpho-topographic and climate controls. *The Cryosphere* 7, 1455–1471.

Rainsley, E., Menviel, L., Fogwill, C.J., Turney, C.S.M., Hughes, A.L.C., Rood, D.H., 2018: Greenland ice mass loss during the Younger Dryas driven by Atlantic Meridional Overturning Circulation feedbacks. *Scientific Reports* 8, 11307.

Rasmussen, S.O., Andersen, K.K., Svensson, A.M., Steffensen, J.P., Vinther, B.M., Clausen, H.B., Siggaard-Andersen, M.L., Johnsen, S.J., Larsen, L.B., Dahl-Jensen, D., Bigler, M., Rothlisberger, R., Fischer, H., Goto-Azuma, K., Hansson, M.E., Ruth, U., 2006: A new Greenland ice core chronology for the last glacial termination. *Journal of Geophysical Research - Atmospheres* 111, D06102.

Rasmussen, S.O., Seierstad, I.K., Andersen, K.K., Bigler, M., Dahl-Jensen, D., Johnsen, S.J., 2008: Synchronization of the NGRIP, GRIP, and GISP2 ice cores across MIS 2 and palaeoclimatic implications. *Quaternary Science Reviews* 27, 18–28.

Reitner, J.M., Ivy Ochs, S., Dreschner-Schneider, R., Hajdas, I., Linner, M., 2016:

Reconsidering the current stratigraphy of the Alpine Lateglacial: Implications of the sedimentary and morphological record of the Lienz area (Tyrol/Austria). *E&G Quaternary Science Journal* 65, 113-144.

Renssen, H., Isarin, R.F.B., 2001: The two major warming phases of the last deglaciation at ∼14.7 and ∼11.5 ka cal BP in Europe: climate reconstructions and AGCM experiments. *Global and Planetary Change* 30, 117–153.

Renssen, H., Mairesse, A., Goosse, H., Mathiot, P., Heiri, O., Roche, D.M., Nisancioglu, K.H., Valdes, P.J., 2015 : Multiple causes of the Younger Dryas cold period. *Nature Geoscience* 8, 946–949.

Roe, G.H., Baker, M.B., Herla, F., 2017: Centennial glacier retreat as categorical evidence of regional climate change. *Nature Geoscience* 10, 95–99.

Schenk, F., Väliranta, M., Muschitiello, F., Tarasov, L., Heikkilä, M., Björck, S., Brandefelt, J., Johansson, A.V., Näslund, J.-O., Wohlfarth, B., 2018: Warm summers during the Younger Dryas cold reversal. *Nature Communications* 9, 1634.

Schimmelpfennig, I., Le Roy, M., Deline, P., Schoeneich, P., Carcaillet, J., Bodin, X., Team, A., 2019: Holocene dynamics of Arsine glacier (Ecrins massif, French Alps) inferred from ^{10}Be dating. INQUA, Dublin. DOI: 10.13140/RG.2.2.10849.86884

Schimmelpfennig, I., Schaefer, J.M., Akçar, N., Koffman, T., Ivy-Ochs, S., Schwartz, R., Finkel, R.C., Zimmerman, S., Schlüchter, C., 2014: A chronology of Holocene and Little Ice Age glacier culminations of the Steingletscher, Central Alps, Switzerland, based on high-sensitivity beryllium-10 moraine dating. *Earth and Planetary Science Letters* 393, 220–230.

Schimmelpfennig, I., Schaefer, J.M., Goehring, B.M., Lifton, N., Putnam, A.E., Barrell, D.J.A., 2012: Calibration of the in situ cosmogenic 14C production rate in New Zealand's Southern Alps. *Journal of Quaternary Science* 27, 671–674.

Schindelwig, I., Akçar, N., Kubik, P.W., Schlüchter, C., 2012: Lateglacial and early Holocene

Mis en forme : Français (France)

dynamics of adjacent valley glaciers in the Western Swiss Alps. *Journal of Quaternary Science* 27, 114–124.

Schwander, J., Eicher, U., Ammann, B., 2000: Oxygen isotopes of lake marl at Gerzensee and Leysin (Switzerland), covering the Younger Dryas and two minor oscillations, and their correlation to the GRIP ice core. *Palaeogeography, Palaeoclimatology, Palaeoecology* 159, 203–214.

Shakun, J.D., Clark, P.U., He, F., Lifton, N.A., Liu, Z., Otto-Bliesner, B.L., 2015: Regional and global forcing of glacier retreat during the last deglaciation. *Nature Commununications* 6, 8059.

Smiraglia, C., Azzoni, R.S., D'Agata, C., Maragno, D., Fugazza, D., Diolaiuti, G.A., 2015: The evolution of the Italian glaciers from the previous data base to the New Italian Inventory. Preliminary considerations and results. *Geografia Fisica e Dinamica Quaternaria* 38, 79–87.

Solomina, O.N., Bradley, R.S., Hodgson, D.A., Ivy-Ochs, S., Jomelli, V., Mackintosh, A.N., Nesje, A., Owen, L.A., Wanner, H., Wiles, G.C., Young, N.E., 2015: Holocene glacier fluctuations. *Quaternary Science Reviews* 111, 9–34.

Vincent, C., Fischer, A., Mayer, C., Bauder, A., Galos, S.P., Funk, M., Thibert, E., Six, D., Braun, L., Huss, M., 2017 : Common climatic signal from glaciers in the European Alps over the last 50 years. *Geophysical Research Letters* 44, 1376-1383.

Vinther, B.M., Clausen, H.B., Johnsen, S.J., Rasmussen, S.O., Andersen, K.K., Buchardt, S.L., Dahl-Jensen, D., Seierstad, I.K., Siggaard-Andersen, M.-L., Steffensen, J.P., Svensson, A., Olsen, J., Heinemeier, J., 2006: A synchronized dating of three Greenland ice cores throughout the Holocene. *Journal of Geophysical Research - Atmospheres* 111, D13102.

Ward, G.K., Wilson, S.R., 1978: Procedures for comparing and combining radiocarbon age determinations: a critique. *Archaeometry* 20, 19–31.

Wittmeier, H.E., Schaefer, J.M., Bakke, J., Rupper, S., Paasche, Ø., Schwartz, R., Finkel, R.C., 2020: Late Glacial mountain glacier culmination in Arctic Norway prior to the Younger Dryas.

Quaternary Science Reviews 245, 106461.

Wurth, G., Niggemann, S., Richter, D.K., Mangini, A., 2004: The Younger Dryas and Holocene climate record of a stalagmite from Hölloch Cave(Bavarian Alps, Germany. *Journal of Quaternary Science* 19, 291–298.

Young, N.E., Briner, J.P., Miller, G.H., Lesnek, A.J., Crump, S.E., Thomas, E.K., Pendleton, S.L., Cuzzone, J., Lamp, J., Zimmerman, S., Caffee, M., Schaefer, J.M., 2020: Deglaciation of the Greenland and Laurentide ice sheets interrupted by glacier advance during abrupt coolings. *Quaternary Science Reviews* 229, 106091.

Young, N.E., Briner, J.P., Schaefer, J., Zimmerman, S., Finkel, R.C., 2019: Early Younger Dryas glacier culmination in southern Alaska: Implications for North Atlantic climate change during the last deglaciation. *Geology* 47, 550–554.

Young, N.E., Schaefer, J.M., Briner, J.P., Goehring, B.M., 2013. A 10Be production-rate calibration for the Arctic. *Journal of Quaternary Science* 28, 515–526.

Figures

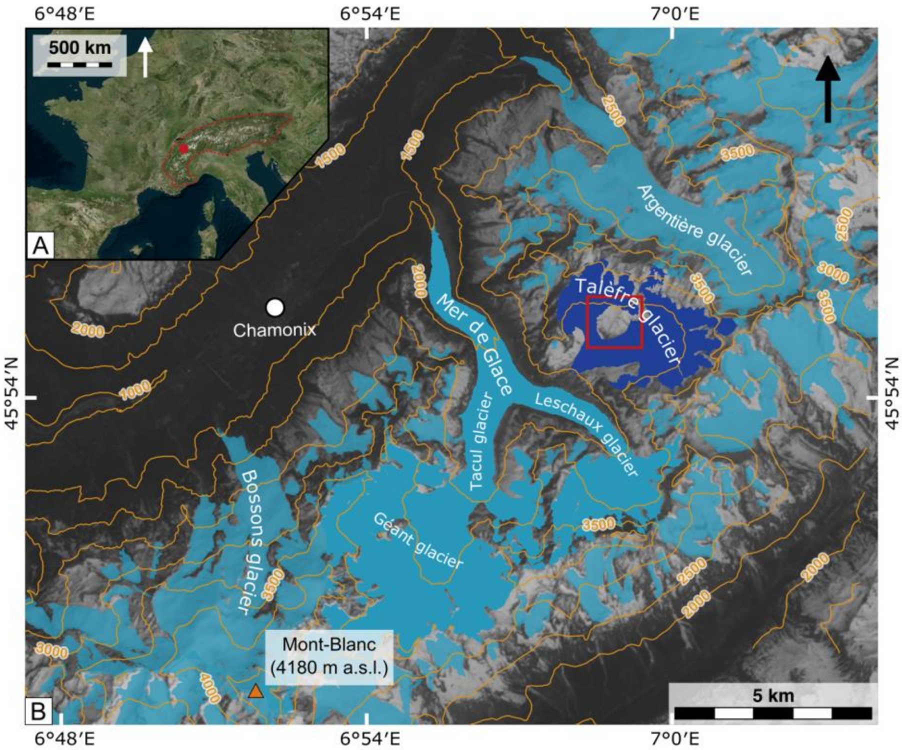

Fig. 1: Location of Talèfre glacier and study area: the "Jardin de Talèfre". (A) Location of the Mont Blanc massif (red dot) in the Alps (red dotted line). (B) The Mont Blanc massif and present-day glacier extents on a Landsat 8 image (April 2015); French glaciers: Gardent et al. (2014); Swiss glaciers: Fischer et al. (2014); Italian glaciers: Smiraglia et al. (2015). Talèfre glacier is highlighted in dark blue, the "Jardin de Talèfre" is located in the red square.

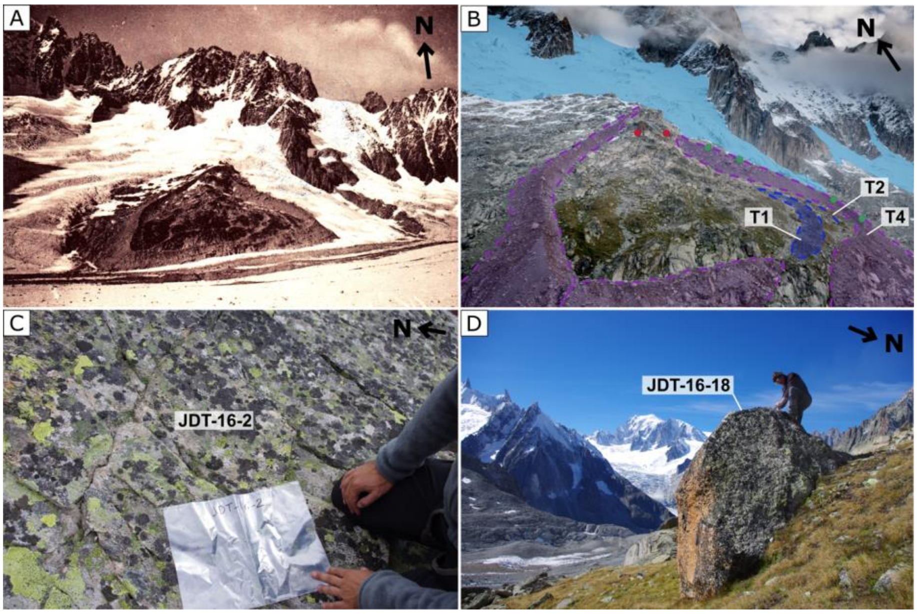

Fig. 2: (A) Photograph~~y~~ of the « Jardin de Talèfre » in 1890 C.E. (source: "Les Amis du Vieux Chamonix"); (B) oblique aerial ~~photography~~ imagery of the “Jardin de Talèfre” in September 2016; Talèfre glacier is highlighted in light blue, sampled moraines T1 and T2 (dark blue) and Holocene moraines, including T4 (purple); bedrock sample locations are shown as red dots and some of the sampled boulders as green dots (photograph~~y~~ by J.F. Buoncristiani); (C) example of sampled bedrock surface; (D) example of sampled boulder on T2 moraine.

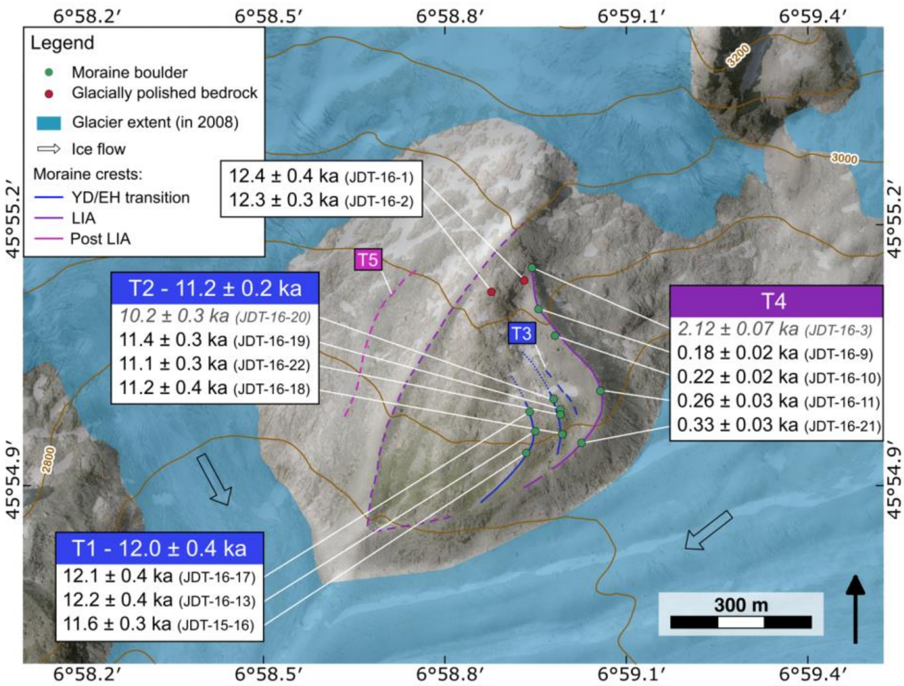

Fig. 3: Moraines and sample locations in the "Jardin de Talèfre", mapped on the 5 m IGN DEM RGE ALTI and aerial images. Present-day glacier extent (in blue) is from Gardent et al. (2014). Dashed lines represent undated moraines, the age of which is assumed according to their relative position and morphology~~appearance~~. Individual surface exposure ages are listed in the white boxes with their analytical uncertainties and mean ages of the landforms in the colored bands (arithmetic means and standard deviations). ~~Outlier~~Outliers are in italic grey font.

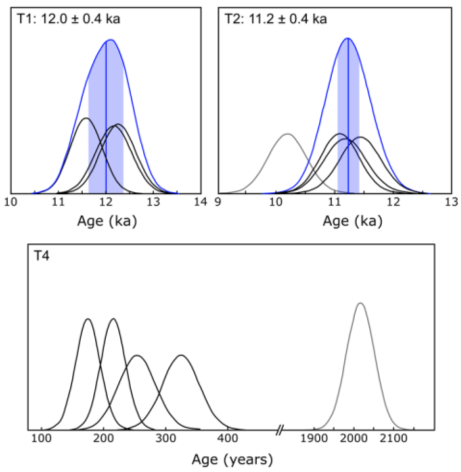

Fig. 4: Probability plots of the individual moraine sample ages (black curves, analytical uncertainty only) from Talèfre glacier. Colored curves, vertical lines and bands represent the summed probability plots, arithmetic means and standard deviations, respectively, corresponding to the age labeled in each box, only calculated for T1 and T2.

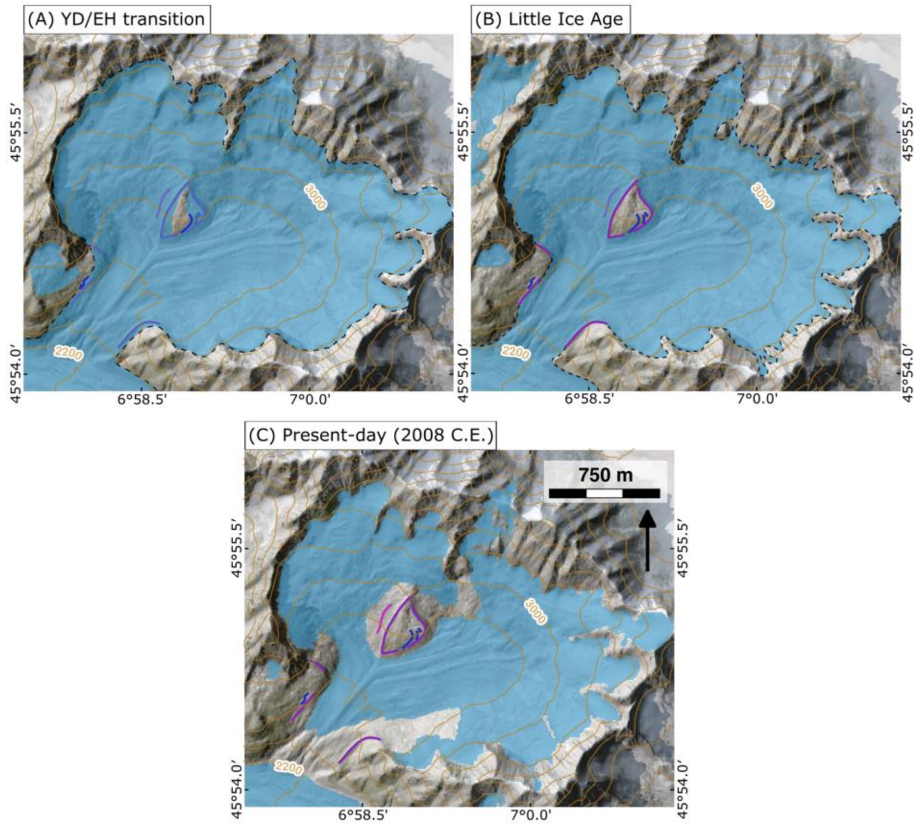

Fig. 5: ~~Estimation~~ Reconstruction of past extents of Talèfre glacier, based on mapping of the preserved moraines and interpretation of ^{10}Be dating, for the (A) during the Younger Dryas/Early Holocene transition (12 ka, stage T1 moraine), (C) LIA maximum and (C) 2008 C.E. (Gardent et al., 2014). Dashed glacier limits correspond to hypothetic extents.

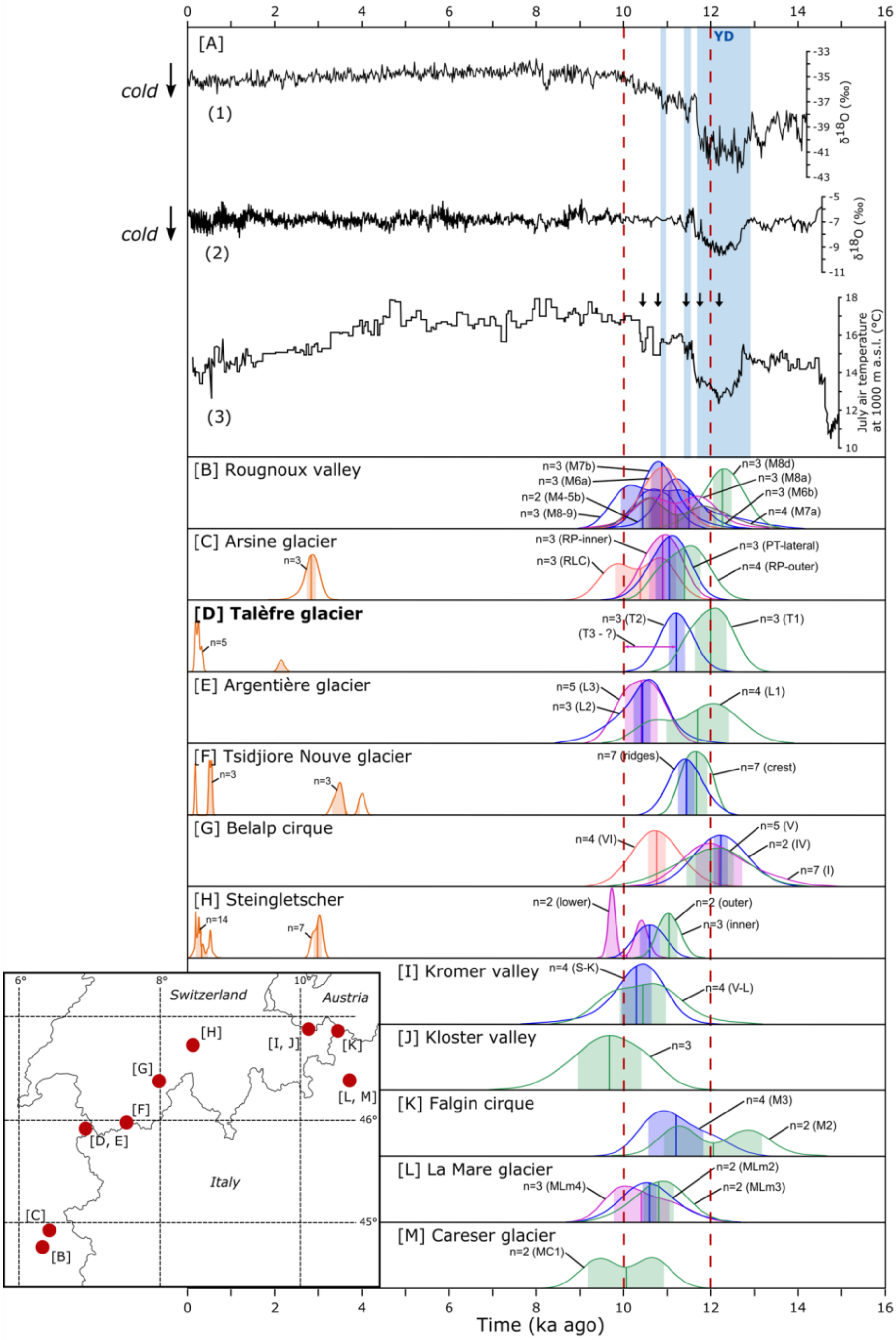

[A]
YD
cold
(1)
(2)
(3)
δ18O (‰)
July air temperature at 1000 m a.s.l. (°C)
[B] Rougnoux valley
[C] Arsine glacier
[D] Talèfre glacier
[E] Argentière glacier
[F] Tsidjiore Nouve glacier
[G] Belalp cirque
[H] Steingletscher
[I] Kromer valley
[J] Kloster valley
[K] Falgin cirque
[L] La Mare glacier
[M] Careser glacier
Switzerland
Austria
Italy
Time (ka ago)

851

Fig. 6: Chronology of culminations of Talèfre glacier based on the ^{10}Be mean ages of the glacial landforms in this study [panel D] compared to independent paleoclimate records [panel A] and to other glacier chronology studies in the Alps also using ^{10}Be moraine dating [panels B to M]. Each moraine is represented by a summed probability curve along with the number of dated boulders (n=x), vertical lines and colored band represent the arithmetic means and standard deviations (1σ), colors represent the stratigraphic order of the moraines (from outer to inner: green, blue, purple, pink). Panel [A]: (1) Oxygen isotope record in Greenland ice core NGRIP (Rasmussen et al., 2006; Vinther et al., 2006), blue bands represent the Younger Dryas and cold peaks during the Early Holocene as identified in the Greenland ice core record, (2) Oxygen isotope record from speleotem fluid inclusion from Milandre cave, Switzerland (Affolter et al., 2019) (3) Stacked chironomid-inferred July air temperature from the Alps (Heiri et al., 2015), black arrows point to peaks mentioned in the main text. Alpine glacier sites in panels [B], [C] and [E] to [M] are presented from east to west with their locations shown by red dots on the map. [B] Rougnoux valley (Hofmann, 2018), [C] Arsine glacier (Schimmelpfennig et al., 2019; Le Roy et al., in prep), [E] Argentière glacier (Protin et al., 2019), [F] Tsidjiore Nouve glacier (Schimmelpfennig et al., 2012), [G] Belalp cirque (Schindelwig et al., 2012), [H] Steingletscher (Schimmelpfennig et al., 2014), [I] Kromer valley (Kerschner et al., 2006; Moran et al., 2016b), [J] Kloster valley (Moran et al., 2016b), [K] Falgin glacier (Moran et al., 2016a), [L] La Mare glacier (Baroni et al., 2017) and [M] Careser glacier (Baroni et al., 2017). Vertical dashed lines delimit the YD/EH transition period between 12 and 10 ka ago.

Tables

Table 1: Characteristics and ^{10}Be measurement details of samples [A] and blanks [B] carried out for this study. Outliers are highlighted by (O). Mean landform ages of T1 and T2 are

indicated with standard deviations and total uncertainties (including the ^{10}Be production rate uncertainty) in parentheses.

Commenté [MOU15]: Marie, add the Artic PR ages

Sample name	Latitude (dd)	Longitude (dd)	Altitude (m a.s.l.)	Thickness (mm)	Shielding factor	Quartz weight (g)	Carrier (mg ^{9}Be)	Associated blank	^{10}Be/^{9}Be x10^{-14}	[^{10}Be] (x10^{4} at.g^{-1})	^{10}Be age (ka)	1σ analytical uncertainty (ka)	1σ total uncertainty (ka)
MORAINE SAMPLES													
T1													11.97 ± 0.36 (0.4)
JDT-16-17	45.91642	6.98233	2825	45	0.9063	24.67	0.3053	15Jan18	44.9 ± 1.4	36.8 ± 1.2	12.14	0.37	0.47
JDT-16-13	45.91604	6.98249	2817	27	0.9635	15.35	0.3072	15Jan18	30.13 ± 0.93	39.8 ± 1.2	12.21	0.36	0.46
JDT-16-16	45.91564	6.98224	2798	22	0.9635	28.65	0.3078	15Jan18	52.3 ± 1.6	37.3 ± 1.2	11.56	0.34	0.42
T2													11.21 ± 0.17 (0.28)
JDT-16-20 (O)	45.91667	6.98301	2835	42	0.9638	26.58	0.3071	15Jan18	42.7 ± 1.4	32.7 ± 1.1	10.15	0.32	0.4
JDT-16-19	45.91647	6.98318	2827	25	0.9638	21.49	0.3070	15Jan18	39.5 ± 1.3	37.4 ± 1.2	11.40	0.34	0.43
JDT-16-22	45.91636	6.98320	2824	24	0.9638	32.44	0.3069	15Jan18	57.6 ± 1.8	36.2 ± 1.1	11.07	0.33	0.41
JDT-16-18	45.91599	6.98324	2805	35	0.9527	20.18	0.3083	15Jan18	34.9 ± 1.2	35.3 ± 1.2	11.15	0.35	0.44
T4													
JDT-16-3 (O)	45.91918	6.98241	2951	20	0.9677	37.83	0.3048	08Dec17	13.43 ± 0.42	7.05 ± 0.23	2.12	0.07	0.09
JDT-16-9	45.91840	6.98260	2923	38	0.9625	31.65	0.3033	08Dec17	1.33 ± 0.11	0.64 ± 0.08	0.18	0.02	0.02
JDT-16-10	45.91788	6.98305	2903	28	0.9625	31.26	0.3017	08Dec17	1.56 ± 0.11	0.78 ± 0.08	0.22	0.02	0.02
JDT-16-11	45.91683	6.98430	2842	26	0.9434	36.61	0.3063	08Dec17	1.88 ± 1.2	0.86 ± 0.07	0.26	0.03	0.03

JDT-16-21	45.91583	6.98377	2796	22	0.9623	33.60	0.3010	08Dec17	2.16 ± 0.12	1.09 ± 0.08	0.33	0.03	0.03
BEDROCK SAMPLES													
JDT-16-1	45.91873	6.98128	2950	32	0.9667	20.09	0.3015	08Dec17	44.2 ± 1.4	44.0 ± 1.4	12.43	0.38	0.48
JDT-16-2	45.91894	6.98219	2943	26	0.9677	17.83	0.3048	08Dec17	38.6 ± 1.1	43.7 ± 1.2	12.31	0.33	0.44

Blanks

Blank name	Carrier (mg ^{9}Be)	^{10}Be/^{9}Be x10^{-14}	Number of ^{10}Be atoms (x10^{4} at)
8Dec17	0.3040	0.338 ± 0.049	6.9 ± 1.0
15Jan18	0.3075	0.348 ± 0.050	7.2 ± 1.0